View metadata, citation and similar papers at core.ac.uk

brought to you by CORE

provided by eScholarship@UMMS

University of Massachusetts Medical School

eScholarship@UMMS

Open Access Articles

Open Access Publications by UMMS Authors

2009-02-26

Supervillin reorganizes the actin cytoskeleton and increases invadopodial efficiency

Jessica Lynn Crowley
University of Massachusetts Medical School

Et al.

Let us know how access to this document benefits you.

Follow this and additional works at: https://escholarship.umassmed.edu/oapubs

 Part of the Cell Biology Commons, and the Medicine and Health Sciences Commons

Repository Citation

Crowley JL, Smith TC, Fang Z, Takizawa N, Luna EJ. (2009). Supervillin reorganizes the actin cytoskeleton and increases invadopodial efficiency. Open Access Articles. https://doi.org/10.1091/mbc.E08-08-0867. Retrieved from https://escholarship.umassmed.edu/oapubs/1923

This material is brought to you by eScholarship@UMMS. It has been accepted for inclusion in Open Access Articles by an authorized administrator of eScholarship@UMMS. For more information, please contact Lisa.Palmer@umassmed.edu.

Molecular Biology of the Cell
Vol. 20, 948–962, February 1, 2009

Supervillin Reorganizes the Actin Cytoskeleton and Increases Invadopodial Efficiency

Jessica L. Crowley, Tara C. Smith, Zhiyou Fang, Norio Takizawa, and Elizabeth J. Luna

Department of Cell Biology and Cell Dynamics Program, University of Massachusetts Medical School, Worcester, MA 01605

Submitted August 22, 2008; Revised November 26, 2008; Accepted December 4, 2008
Monitoring Editor: Joan Brugge

Tumor cells use actin-rich protrusions called invadopodia to degrade extracellular matrix (ECM) and invade tissues; related structures, termed podosomes, are sites of dynamic ECM interaction. We show here that supervillin (SV), a peripheral membrane protein that binds F-actin and myosin II, reorganizes the actin cytoskeleton and potentiates invadopodial function. Overexpressed SV induces redistribution of lamellipodial cortactin and lamellipodin/RAPH1/PREL1 away from the cell periphery to internal sites and concomitantly increases the numbers of F-actin punctae. Most punctae are highly dynamic and colocalize with the podosome/invadopodial proteins, cortactin, Tks5, and cdc42. Cortactin binds SV sequences in vitro and contributes to the formation of enhanced green fluorescent protein (EGFP)-SV induced punctae. SV localizes to the cores of Src-generated podosomes in COS-7 cells and with invadopodia in MDA-MB-231 cells. EGFP-SV overexpression increases average numbers of ECM holes per cell; RNA interference-mediated knockdown of SV decreases these numbers. Although SV knockdown alone has no effect, simultaneous down-regulation of SV and the closely related protein gelsolin reduces invasion through ECM. Together, our results show that SV is a component of podosomes and invadopodia and that SV plays a role in invadopodial function, perhaps as a mediator of cortactin localization, activation state, and/or dynamics of metalloproteinases at the ventral cell surface.

INTRODUCTION

During metastasis, tumor cells invade the surrounding extracellular matrix (ECM), migrate into the bloodstream, and traverse endothelial barriers at secondary sites in distant organs (Condeelis *et al*., 2005). ECM degradation, in vitro, involves specialized membrane-associated F-actin structures known as podosomes and invadopodia (Weaver, 2006; Linder, 2007; Gimona *et al*., 2008; Machesky *et al*., 2008). Podosomes are endogenously found in cell types that cross tissue boundaries or are involved in tissue remodeling, e.g., leukocytes and osteoclasts, respectively (Gimona *et al*., 2008). Although podosomes contain many focal adhesion proteins and may mediate dynamic cell–ECM attachments, they are distinguishable from focal adhesions, which are ECM- and integrin-associated complexes that promote cell migration in fibroblasts (Zaidel-Bar *et al*., 2004; Evans and Matsudaira, 2006; Lo, 2006; Romer *et al*., 2006; Spinardi and Marchisio, 2006; Block *et al*., 2008; Broussard *et al*., 2008). Podosomes turn over much faster than do focal adhesions and contain cores of actin filaments that are surrounded by rings of vinculin and other focal adhesion proteins (Gavazzi *et al*., 1989; Ochoa *et al*., 2000; Destaing *et al*., 2003; Evans and Matsudaira, 2006). Electron micrographs of podosomes in Rous sarcoma virus-transformed fibroblasts show that the dense microfilamentous material in the core surrounds a central invaginating membrane tubule (Nitsch *et al*., 1989; Ochoa *et al*., 2000). Invadopodia mediate ECM degradation, are larger and longer-lived than podosomes, and are characterized by surface protrusions and large membrane invaginations (Chen and Wang, 1999; Baldassarre *et al*., 2003; Yamaguchi and Condeelis, 2007; Stylli *et al*., 2008).

Recent studies indicate many functional and compositional similarities between podosomes and invadopodia. Both these structures have been associated with secretion of matrix metalloproteinases (MMPs) and endocytosis of degraded matrix components (Ochoa *et al*., 2000; Baldassarre *et al*., 2003; Clark and Weaver, 2008). Also, both structures contain several proteins in common—including cortactin, Tks5/FISH, and Cdc42—in addition to many proteins also found at focal adhesions (Seals *et al*., 2005; Linder, 2007; Yamaguchi and Condeelis, 2007; Block *et al*., 2008). Current nomenclature is to use the term "invadopodia" for invasive structures in tumor cells and to use "podosome" for the invasive/adhesive structures in transformed fibroblasts and in cells—such as leukocytes, osteoclasts, and endothelial and smooth muscle cells—with endogenous or inducible podosomes (Gimona *et al*., 2008). However, vascular smooth muscle cells invade ECM, and tumor cells contain podosome-like, dynamic "preinvadopodial complexes" with short lifetimes that mature into longer lived invadopodia (Yamaguchi *et al*., 2005; Furmaniak-Kazmierczak *et al*., 2007). In addition, invadopodium formation involves sequential stages of cortactin recruitment to membranes, membrane type (MT) 1–MMP accumulation, matrix degradation, and

This article was published online ahead of print in *MBC in Press* (http://www.molbiolcell.org/cgi/doi/10.1091/mbc.E08–08–0867) on December 24, 2008.

Address correspondence to: Elizabeth J. Luna (elizabeth.luna@umassmed.edu).

Abbreviations used: ECM, extracellular matrix; ERK, extracellular signal-regulated kinase; MMP, matrix metalloproteinase; pTyr, phosphotyrosine; SmAV, smooth muscle isoform of supervillin; SV, supervillin.

© 2009 by The American Society for Cell Biology

cortactin dissociation (Artym *et al*., 2006). Thus, the distinction between "podosomes" and "invadopodia" may be as much temporal as compositional, i.e., invasion structures may arise from more dynamic podosome-like precursors in both normal tissues and tumors (Linder and Aepfelbacher, 2003; Gimona *et al*., 2008). Here, we use the current nomenclature for podosomes and invadopodia and refer to undefined structures as "actin punctae."

Supervillin (SV) is one of the largest members of the villin/gelsolin family of actin-organizing proteins, which have both overlapping and distinct functions (Silacci *et al*., 2004; Archer *et al*., 2005; Khurana and George, 2008). Villin is associated with precancerous morphological changes in epithelia, and gelsolin is required for the formation and degradative activity of osteoclast podosomes; gelsolin also promotes cancer cell invasion and motility (MacLennan *et al*., 1999; Chellaiah *et al*., 2000; De Corte *et al*., 2002; Rieder *et al*., 2005; Van den Abbeele *et al*., 2007). Nonmuscle SV copurifies from neutrophil plasma membranes as a component of a lipid raft-like complex that also includes heterotrimeric G proteins, Src family kinases, and MT6-MMP (Nebl *et al*., 2002), all of which are involved in tumorigenesis and matrix degradation (Mareel and Leroy, 2003; Ingley, 2008; Sohail *et al*., 2008). A smooth muscle isoform of SV, called SmAV, localizes to phorbol ester-induced podosomes in A7r5 cells with F-actin, nonmuscle myosin IIB, and extracellular signal-regulated kinases (ERKs) 1/2 (Gangopadhyay *et al*., 2004). SmAV is required for normal ERK1/2 activation downstream of phenylephrine signaling in ferret aorta (Gangopadhyay *et al*., 2004), but the functionality of SV isoforms in the formation of podosome-like structures has not been explored.

Based on its biochemical characteristics, SV is well positioned for a role in mediating alterations in the actin cytoskeleton at membranes. SV cofractionates with membranes and binds very tightly to the membrane bilayer, resisting extraction with buffered solutions at pH <12 (Pestonjamasp *et al*., 1997; Nebl *et al*., 2002; Oh *et al*., 2003). One site of membrane attachment is associated with SV amino acids 342–571 (SV342-571), which interact with the LIM domains of the focal adhesion proteins, thyroid receptor-interacting protein (TRIP) 6/zyxin-related protein 1, and lipoma-preferred partner (Takizawa *et al*., 2006). SV also binds avidly to F-actin at three sites through which it can either bundle or cross-link actin filaments; to nonmuscle myosins IIA and IIB; to the long isoform of myosin light chain kinase; and to calponin (Chen *et al*., 2003; Takizawa *et al*., 2007), a negative regulator of podosome formation in smooth muscle cells (Gimona *et al*., 2003).

SV potentiates a process that negatively regulates focal adhesion function. Overexpressed SV decreases cell adhesion to fibronectin, whereas RNA interference (RNAi)-mediated SV down-regulation increases cell attachment (Takizawa *et al*., 2006). Sequences within the SV N terminus (SV1-171) disrupt stress fibers by inducing apparent hypercontractility of myosin II (Takizawa *et al*., 2006, 2007). Another SV sequence (SV342-571) counteracts stress fiber and large focal adhesion formation or stability through the interaction with TRIP6 (Takizawa *et al*., 2006). However, phalloidin staining of cytoplasmic F-actin is observed even after disruption of stress fibers in cells expressing elevated levels of SV or SV342-571 (Wulfkuhle *et al*., 1999; Takizawa *et al*., 2006). The nature of these phalloidin-stained structures has never been explored.

The mechanism by which SV and TRIP6 regulate adhesion also is imperfectly understood. Most investigations have focused on the roles of these proteins in "inside-out" signaling through other proteins on the cytoplasmic sides of focal adhesions (Yi *et al*., 2002; Lai *et al*., 2005, 2007; Bai *et al*., 2007; Takizawa *et al*., 2007). An alternative, nonmutually exclusive hypothesis, tested in this study, is that SV induces the loss of focal adhesion function by promoting the formation of podosomes, invadopodia, and ECM degradation.

MATERIALS AND METHODS

Antibodies, Reagents, and Constructs

Mouse monoclonal anti-vinculin (hVIN1) and anti-gelsolin (clone GS-2C4) antibodies were from Sigma-Aldrich (St. Louis MO), as was affinity-isolated rabbit anti-hemagglutinin (HA) tag. Mouse monoclonal anti-cortactin (4F11) and anti-actin (clone C4) antibodies were from Millipore (Billerica, MA). Mouse monoclonal anti-phosphotyrosine (pTyr-100) and anti-myc (71D10) antibodies were from Cell Signaling Technology (Danvers, MA). Mouse monoclonal anti-phospho-focal adhesion kinase (FAK) (pY397) antibody was from BD Biosciences (Franklin Lakes, NJ). AlexaFluor 488- and 568-conjugated secondary antibodies against rabbit and mouse immunoglobulin Gs (IgGs), and fluorescein- and Texas Red-conjugated phalloidin were from Invitrogen (Carlsbad, CA) and used at 1:2000 dilution. Affinity-purified rabbit polyclonal antibodies against SV (H340) and lamellipodin (3917) have been described previously (Krause *et al*., 2004; Nebl *et al*., 2002; Oh *et al*., 2003).

EGFP-C1 and EGFP-SV vectors were described previously (Wulfkuhle *et al*., 1999). An untagged version of bovine SV was made by cloning the full-length SV cDNA into the KpnI and XbaI sites of pTracer-CMV (Invitrogen) (Wulfkuhle *et al*., 1999). His-tagged cortactin(ΔSH3, amino acids 1–506) was generated from pdsRed-cortactin (gifted by Dr. Alan S. Mak, Queen's University, Kingston, ON, Canada) (Webb *et al*., 2006a) after digestion with BglII and cloning into pET30a vector (Invitrogen). Y527F-Src was from the Harold Varmus laboratory (National Institutes of Health, Bethesda, MD). Myc-tagged Tks5 (myc-Tks5) (Lock *et al*., 1998) and HA-tagged Cdc42 (Shinjo *et al*., 1990) (HA-Cdc42), both in the pEF-BOS expression vector (Mizushima and Nagata, 1990), were kind gifts from Drs. Sara Courtneidge (Burnham Institute for Medical Research, La Jolla, CA) and Dr. Kozo Kaibuchi (Nagoya University, Nagoya, Japan), respectively. EGFP-MT1-MMP was from Dr. Maria C. Montoya (Spanish Nacional Cancer Research Center [CNIO], Madrid, Spain) (Galvez *et al*., 2002; Bravo-Cordero *et al*., 2007).

Immunoblotting

Whole cell lysates were prepared in 1% SDS, phosphate-buffered saline (PBS), 1 mM phenylmethylsulfonyl fluoride (PMSF), and a protease inhibitor cocktail containing: 1 μg/ml aprotinin, 1 μM antipain, 2 μM ALLM (calpain inhibitor II), 1 mM benzamidine, 10 μM E64, 1 μM leupeptin, and 1 μM pepstatin A. For each sample, 40 or 50 μg of protein, as determined by bicinchoninic acid protein assay (Pierce Chemical, Rockford, IL), were run on SDS-polyacrylamide gels (Laemmli, 1970), transferred to nitrocellulose membranes (Towbin *et al*., 1979), and probed with primary antibodies against supervillin (0.2–0.4 μg/ml) and gelsolin (1:5000); β-actin (1:5000 antibody dilution) was used as a loading control. Horseradish peroxidase-conjugated goat anti-mouse or goat anti-rabbit secondary antibodies (Jackson ImmunoResearch Laboratories, West Grove, PA), diluted 1:20,000, were detected by Pierce SuperSignal WestPico chemiluminescence. Band densities were determined using ImageJ (Rasband, National Institutes of Health, Bethesda, MD; http://rsb.info.nih.gov/ij/). EGFP-SV expression levels were determined by comparing band intensities with endogenous SV and correcting for transfection efficiency.

Cell Culture and Transfection

COS7-2 cells, a highly transfectable clone of COS7 (Kowalczyk *et al*., 1997), were a generous gift from Dr. Kathleen J. Green (Northwestern University, IL). COS7 cells were grown in high glucose DMEM (11995; Invitrogen) supplemented with 10% fetal calf serum (FCS) for $\leq$20 passages. MDA-MB-231 breast carcinoma cells were obtained from American Type Culture Collection (Manassas, VA) and from the Tissue Culture Shared Resource of the Lombardi Cancer Center (courtesy of Dr. Susette Mueller, Georgetown University, Washington, DC). G418-resistant MDA-MB-231 cells that stably overexpress wild-type c-Src (MDA-MB-231/WT Src cells) were a kind gift from Dr. Toshiyuki Yoneda (University of Texas Health Science Center, San Antonio, TX) and Dr. S. Mueller (Myoui *et al*., 2003; Bowden *et al*., 2006). MDA-MB-231 cells without and with WT c-Src overexpression were grown in DMEM supplemented with 10% FCS and 2 mM L-glutamine (25030; Invitrogen). Cultured cells for immunoblots were generously supplied by Drs. G. Sluder (primary human foreskin fibroblasts and hTERT-RPE1; Clontech, Mountain View, CA), L. Languino (LNCaP), K. C. Balaji (LNCaP, C4-2, and DU-145), and A. Mercurio (MCF10A series), all from University of Massachusetts Medical School.

Transfection methods have been described previously (Takizawa *et al*., 2006). Briefly, for plasmids, COS7 cells were transfected using Effectene

Transfection Reagent (QIAGEN, Valencia, CA) for 24 h with the Y527F-Src, HA-Cdc42, and myc-Tks5 plasmids or for 24 or 48 h with the EGFP-SV plasmid. For small interfering RNAs (siRNAs), COS7 cells were transfected with Lipofectamine 2000 (Invitrogen). MDA-MB-231/WT Src cells were transfected using the Nucleofector system (Amaxa Biosystems, Gaithersburg, MD), according to manufacturer's instructions. Briefly, for each Nucleofection, 1×10^6 adherent cells were trypsinized, rinsed with Dulbecco's PBS, modified (14190; Invitrogen), resuspended with 100 μl of solution V and with either 40 nM Stealth siRNA or 2 μg of plasmid, and treated using program X13. Cells treated with siRNA were incubated for 4 d before experiments, whereas cells treated with plasmid were incubated for 2 d.

The double-stranded (ds)RNAs targeting COS7 cell SV have been described previously (Takizawa *et al*., 2007). Two dsRNAs targeting human SV were made as Stealth duplexes (Invitrogen): human (h)SV1, 5′-CAGCCAUAAGGAAUCUAAAUAUGCU-3′ (coding nucleotides 1680-1704); and hSV2, 5′-GCGAUGUUUGCUGCUGGAGAGAUCA-3′ (coding nucleotides 2026-2050). The Stealth duplex sequence 5′-GAACUAUGAAGGACCACCAGAGAUA-3′ was used as a control dsRNA. A dsRNA targeting human gelsolin was also made as a Stealth Duplex with the sequence 5′-CAGTTCTATGGAGGCGACAGCTACA-3′ (coding nucleotides 1460-1484). Two dsRNAs targeting primate cortactins were made as Stealth duplexes: CT1 5′-UCUUGUUCCACACCAAAUUUCCCUC-3′ and CT2 5′-GAGGGAAAUUUGGUGUGGAACAAGA-3′.

Recombinant Protein Purification and in Vitro Pull-Down Assay

Glutathione transferase (GST)-SV fusion fragment proteins were expressed after isopropyl β-D-thiogalactoside (IPTG) induction in BL21(DE3)pLysS cells and purified with glutathione-Sepharose as described previously (Chen *et al*., 2003). His-cortactin(ΔSH3) was expressed after induction by IPTG and purified by using nickel-nitrilotriacetic acid Agarose (QIAGEN). Eluted proteins were dialyzed in dialysis buffer (50 mM Tris, pH 8.0, 150 mM NaCl, 1 mM dithiothreitol [DTT], and 10% glycerol). Dialyzed proteins were frozen quickly in liquid nitrogen and stored at −80°C.

Purified GST-SV fragments were mixed with His-cortactin(ΔSH3) in binding buffer (50 mM Tris, pH 8.0, 300 mM NaCl, 1% Triton X-100, 1 mM DTT, 10% glycerol, 1 mM PMSF, and protease inhibitor cocktail) and incubated with glutathione-Sepharose beads for 1 h at 4°C with shaking. The mixtures were then washed five times with binding buffer followed by centrifugation at 3000 rpm for 2 min. Beads were resuspended in 2× SDS sample buffer and heated to 95°C for 5 min. Proteins were separated by SDS-PAGE and transferred to a nitrocellulose membrane. His-cortactin(ΔSH3) was identified by immunoblotting with monoclonal anti-His antibody (clone 27E8; Cell Signaling Technology).

Live Cell Imaging

COS7 cells transfected with EGFP-SV were cultured on 22-mm square coverslips and sealed into chambers with DMEM, 10% FCS, and 10 mM HEPES, without phenol red. After temperature equilibration in a Plexiglas environmental chamber heated to 37°C, images focused on the ventral cell surface were acquired for EGFP, by using an HCX PL Apo 63× 1.32 numerical aperture (NA) oil immersion objective lens on a DMIRE 2 inverted microscope (Leica Microsystems, Allendale, NJ), a Retiga Exi cooled charge-coupled device (CCD) camera (QImaging Corp., Burnsby BC, Canada), and OpenLab 3.5.2 software (Improvision, Waltham, MA). Images were processed with OpenLab to enhance contrast and to generate movie files. Labels and movie titles were added with Adobe Photoshop (Adobe Systems, San Jose, CA) and QuickTime Pro (Apple, Cupertino, CA).

Immunofluorescence

Cells were fixed for 10 min with 4% paraformaldehyde in PBS and permeabilized for 5 min with 0.2% Triton X-100 in PBS before blocking for 30 min with 1% bovine serum albumin (BSA), 0.5% Tween 20 in PBS and immunostaining. Depending on the experiment, cells were stained for cortactin (1:200 dilution), phosphotyrosine (pTyr; 1:100), myc (1:200), HA (1:100), vinculin (1:200), phosphorylated FAK 397 (pFAK; 1:100), α-actinin (1:200), and/or anti-SV (1:200). F-actin was visualized with phalloidin conjugated to Texas Red or fluorescein (Invitrogen). Slides were analyzed with a 40× or 100× Plan-NeoFluor oil immersion objective (NA 1.3) on a Zeiss Axioskop fluorescence microscope, a RETIGA CCD camera (QImaging), and OpenLab 3.5.2 software (Improvision). Images were adjusted for contrast and brightness, and merged images were assembled using Adobe Photoshop software (Adobe Systems). For Z-series, images were acquired with a 100× HCX PLAN APO objective lens (NA 1.35) by using step sizes of 0.2 μm on a DM IRE 2 inverted Leica microscope (Leica Microsystems, Bannockburn, IL) with a Retiga Exi cooled CCD camera (QImaging) and OpenLab software. Images were deconvolved using Volocity software (Improvision). Z-series also were obtained with a 100× Plan Apo objective lens (NA 1.4) by using a Solamere CSU10 spinning disk confocal microscope (Solamere Technical Group, Salt Lake City, UT) on a Nikon Eclipse TE-2000 microscope (Nikon Instruments, Melville, NY) and a Roper Scientific CoolSNAP HQ2 camera (Photometrics, Tucson, AZ).

Gelatin-coated Coverslips

The preparation of fluorescently labeled gelatin-coated coverslips was carried out as described previously (Bowden *et al*., 2001). Briefly, 2.5% gelatin, 225 bloom (type B; Sigma-Aldrich) was conjugated with tetramethylrhodamine-5(and-6)-isothiocyanate ([TRITC] T-490; Invitrogen), dialyzed extensively to remove unbound dye, and stored in PBS with 2% sucrose. TRITC-gelatin (200 μl) was heated to 45°C and spread on ethanol-cleaned coverslips (22-mm square). Excess gelatin was removed, and coverslips were inverted onto chilled 0.5% glutaraldehyde in PBS for 15 min. Coverslips were then washed with PBS, and unreacted aldehyde groups were quenched with 5 mg/ml sodium borohydride for 5–10 min. After washing with PBS, coverslips were then sterilized briefly with 70% ethanol and incubated at 37°C in serum-free DMEM for 1 h before plating cells. Cells in complete DMEM then were incubated for 6 h on the gelatin and fixed with 4% paraformaldehyde, as described above.

Matrigel Invasion Assays

Cell invasion assays were performed using BioCoat Matrigel invasion chambers (354480; BD Biosciences), according to the manufacturer's instructions. Briefly, $\sim 5 \times 10^4$ siRNA-treated MDA-MB-231/WT Src cells in serum-free DMEM were added to the upper wells of invasion chambers that contained DMEM with 10% serum in the bottom wells. Cells were allowed to migrate for 20 h, and then cells remaining on the top side of the filter were removed with moistened cotton swabs. Migrated cells were fixed and stained with the HEMA 3 Stain Set (Fisher Scientific, Kalamazoo, MI). Five representative images were taken from each insert with 10× magnification. Cells from the Matrigel inserts were counted using the Cell Counterplugin for ImageJ. Cells from control inserts were counted using the Analyze Particles command in ImageJ after using the Threshold and Watershed commands to identify individual cells. Invasion indices were determined as ratios of cells migrating in the presence versus absence of Matrigel to control for changes in cell motility and by normalizing experimental invasion indices against the mean value obtained for cells treated with control siRNA.

Fluorescence-activated Cell Sorting (FACS) Analyses

The total amounts of cortactin in COS7 cells expressing EGFP or EGFP-SV were assayed after lifting 1×10^6 cells from plates with 0.1% trypsin, 0.4 mg/ml EDTA. The cells were washed twice with PBS and fixed with 2% paraformaldehyde in PBS for 20 min at room temperature with rotation in a 1.5-ml tube. Fixed cells were washed once and made permeable with 0.1% Triton X-100 in PBS for 5 min at room temperature with rotation. After blocking for 30 min with sterile-filtered 4% FBS, 0.05% sodium azide, PBS, the cells were incubated for another 30 min on ice in blocking buffer containing either 0.67 μg/ml mouse anti-cortactin antibody or control mouse IgG1 (Leinco Technologies, St. Louis, MO). Cells were washed three times with blocking buffer and then incubated for 15 min on ice with secondary antibody, AlexaFluor 647-conjugated goat anti-mouse IgG F(ab_2) (1:5000; Invitrogen). The cells were washed three times with blocking buffer and resuspended into 0.5 ml of PBS containing 0.5% BSA in Falcon tubes for FACS analysis.

Statistical Analyses

Statistical significance was assessed using InStat 3 for Macintosh (GraphPad Software, San Diego, CA). Unless otherwise stated, two-tailed p values were determined by one-way analysis of variance with a Tukey–Kramer or Student–Newman–Keuls multiple comparisons post test. As noted in figure legends, some pairs of groups also were compared using unpaired *t* tests.

RESULTS

SV Promotes Restructuring of the Actin Cytoskeleton

SV Overexpression Increases F-Actin Punctae. Increased levels of SV decrease the numbers of COS7 cells containing stress fibers (Takizawa *et al*., 2006). Compared with overexpressed EGFP alone (Figure 1A, a–c), overexpression of either EGFP-tagged SV (EGFP-SV) (Figure 1A, d–f) or untagged SV (Figure 1A, g–i) increases the numbers of F-actin punctae (Figure 1A, e and h vs. b, insets). These punctae, which are $\sim$0.5 μm in diameter, can be either round or irregularly shaped. They are prominent at the ventral surfaces of cells expressing EGFP-SV but are also found near nuclei, especially in EGFP-expressing control cells (Supplemental Figure S1). In wide-field fluorescence (Figure 1A), the mean numbers of ventral F-actin punctae in cells expressing EGFP-SV (Figure 1B) or untagged SV (Figure 1C) increase approximately sevenfold, compared with mock-transfected cells or cells expressing only EGFP, indicating

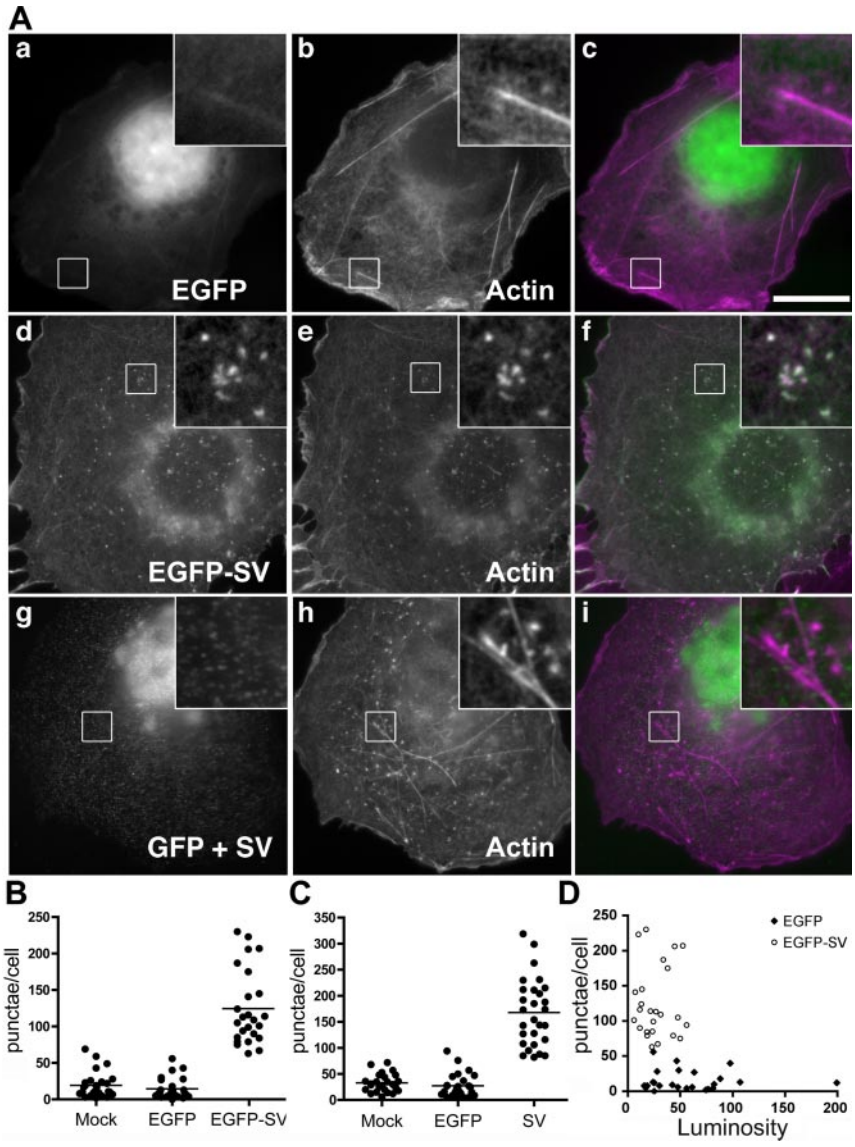

Figure 1. Overexpression of EGFP-SV in COS7 cells increases the numbers of cytoplasmic F-actin punctae. (A) COS7 cells were transfected for 48 h with vectors encoding EGFP (a–c), EGFP-SV (d–f), or GFP plus untagged supervillin (g–i). Cells were fixed and stained for F-actin using Texas Red phalloidin (b, e, and h). Bar, 20 μm. Insets enlarged fourfold. Overlap in white. (B and C) F-actin punctae were counted in untransfected cells after a mock treatment with transfection agent alone, or in cells expressing EGFP, EGFP-SV, or GFP as a marker for untagged SV. Distributions of individual counts and their means are shown. Both EGFP-SV and untagged SV differed from controls, $p \leq 0.001$, $n = 25–28$/group. (D) The relative amounts of EGFP (closed symbols) or EGFP-SV (open symbols) in individual cells were estimated from total luminosities of widefield microscopic images. The plot shows the number of F-actin punctae per cell versus luminosity. EGFP-SV expression levels were 12.5 ± 0.7 (mean ± SD; $n = 3$) times that of endogenous SV. At these expression levels, no significant trend was detected for either data set.

specificity for SV sequences. The increase in ventral F-actin punctae in EGFP-SV–transfected cells was not due solely to protein expression levels because even with very high expression of EGFP, the number of these punctae does not increase to levels seen with EGFP-SV (Figure 1D). This increase in ventral F-actin punctae is apparently a gain of function because RNAi-mediated reduction of endogenous SV to ~20 ± 5% of normal levels does not significantly reduce the low background numbers of F-actin punctae in COS7 cells (data not shown).

Most EGFP-SV Punctae Are Dynamic, but These Structures Are Probably Heterogeneous in Nature. In live cell imaging, ~94% of the EGFP-SV punctae in the cell periphery were highly dynamic and short lived (Figure 2 and Supplemental Video 1). Although occasional movements of ~1.0 μm/s were seen, the instantaneous velocities of these punctae averaged 0.36 ± 0.05 μm/s (mean ± SEM; $n = 19$) over their lifetimes of 2.9 ± 0.3 min (mean ± SEM, $n = 93$) (Figure 2, A and B). These dynamic short-lived punctae moved both toward and away from the cell periphery (Figure 2A, arrowheads; and Supplemental Video 1). The ~6% of the EGFP-SV punctae that were longer lived exhibited lifetimes of at least 30.5 ± 1.6 min (mean ± SEM; $n = 6$) (Figure 2B) and were largely restricted in localization (Figure 2C), with signal intensities that could vary over time (Figure 2A, double arrows). Other longer lived punctae tumbled in place, as though they might be associated with larger, vesicular structures and exhibited sporadic, rapid movements (Figure 2A, arrow; and C). The mean instantaneous velocity of EGFP-SV punctae is most consistent with directional movements propelled by kinesins (~0.5 μm/s), but the variable directionalities and the range of observed velocities suggest the possibility of multiple propulsion mechanisms, including actin comet tails (~0.17 μm/s), myosin Vb (0.22 μm/s), and dynein (~0.9 μm/s) (Porter *et al*., 1987; Woehlke *et al*., 1997; Benesch *et al*., 2002; Toba and Toyoshima, 2004; Paluch *et al*., 2006; Watanabe *et al*., 2006).

EGFP-SV Punctae Contain Podosome Markers, but Not Focal Adhesion Proteins. The lifetimes and dynamic behavior of most EGFP-SV punctae are reminiscent of podosomes or invadopodial precursors (Yamaguchi *et al*., 2005; Evans and Matsudaira, 2006). Although the local-

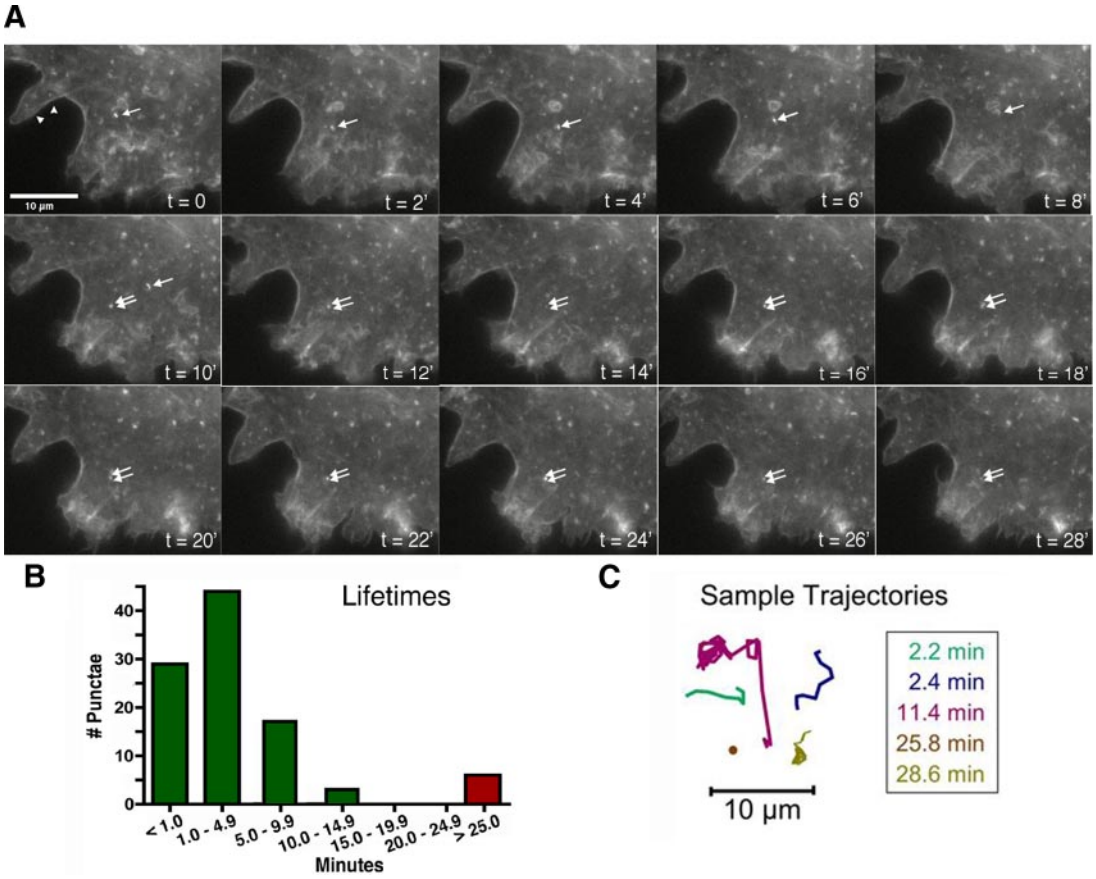

Figure 2. Most EGFP-SV punctae are dynamic and short lived; a few are longer lived and relatively stable. (A) Time-lapse sequence of EGFP-SV punctae in COS7 cells on glass coverslips from Supplemental Video 1. Images were taken every 12 s for 60 min. Bar, 10 μm. Examples of short-lived (arrowheads) and long-lived (arrows) punctae are indicated. (B) Distribution of individual punctae lifetimes; n = 99. (C) Sample trajectories of EGFP-SV punctae with associated lifetimes.

ization of some punctae above the ventral cell surface (Supplemental Figure 1) argues against a 1:1 identity with podosomes, most ventral EGFP-SV punctae do colocalize with podosome/invadopodial proteins (Figure 3). For example, ~91% of the EGFP-SV punctae colocalize with endogenous cortactin (Figure 3, A–C, boxes), a protein required for the formation and function of invadopodia (Bowden *et al*., 1999; Artym *et al*., 2006; Clark *et al*., 2007; Ayala *et al*., 2008; Clark and Weaver, 2008). Also, ~75 and ~50%, respectively, of the EGFP-SV punctae associate with coexpressed myc-Tks5/FISH (Figure 3, D–F) and HA-Cdc42 (Figure 3, G–I), other proteins important for invadopodial function (Nakahara *et al*., 2003; Courtneidge *et al*., 2005; Yamaguchi *et al*., 2005). Approximately 27% of the EGFP-SV punctae contain endogenous phosphotyrosine (Figure 3, J–L), a marker for invadopodia, tyrosine kinase-associated intracellular vesicles, and focal adhesions (Zamir *et al*., 1999; Bowden *et al*., 2006; Sandilands and Frame, 2008). By contrast, only ~3 or ~5%, respectively, of the EGFP-SV punctae colocalize with vinculin or pFAK (Figure 3, M–R), focal adhesion proteins that are present as rings in podosomes but absent from most invadopodia (Bowden *et al*., 2006; Machesky *et al*., 2008). Most of the overlap between EGFP-SV and vinculin and pFAK is at focal adhesions, as reported previously (Figure 3, M–R, arrows) (Wulfkuhle *et al*., 1999; Takizawa *et al*., 2006).

SV Causes a Redistribution of Cortactin. Because EGFP-SV reorganizes F-actin and overlaps extensively at punctae with cortactin, a protein that organizes actin at lamellipodial ruffles and is required for podosomes and invadopodia (Buday and Downward, 2007; Ammer and Weed, 2008; Weaver, 2008), we investigated cortactin localization in cells expressing EGFP-SV (Figure 4). In mock-transfected cells and in cells expressing EGFP alone for 48 h, ~70% (50–109 cells/experiment; n = 3) of the cells exhibit areas of contiguous, ≥20-μm-long cortactin staining at their peripheries (Figure 4A, arrowheads; and B), as described originally (Wu and Parsons, 1993). By contrast, only 33.1 ± 5.7% (~50 cells/experiment; n = 6; $p < 0.0001$) of cells overexpressing EGFP-SV contained strong contiguous peripheral cortactin staining by 48 h after transfection (Figure 4A, d–f, arrows; and B); slight decreases were observed after only 24 h (data not shown). Cortactin was apparently redistributed to the cell interior, as opposed to being differentially stabilized or cleaved by calpain (Perrin *et al*., 2006), because FACS analyses showed no changes in total amounts of cellular cortactin with increasing expression of either EGFP or EGFP-SV (Figure 4C).

Other Lamellipodial Markers Also Are Displaced. To determine whether EGFP-SV promotes the selective redistribution of cortactin, we also monitored two other proteins characteristically concentrated at lamellipodia, lamellipodin/RAPH1/PREL1 (Figure 5, A–C) (Krause *et al*., 2004) and filamin

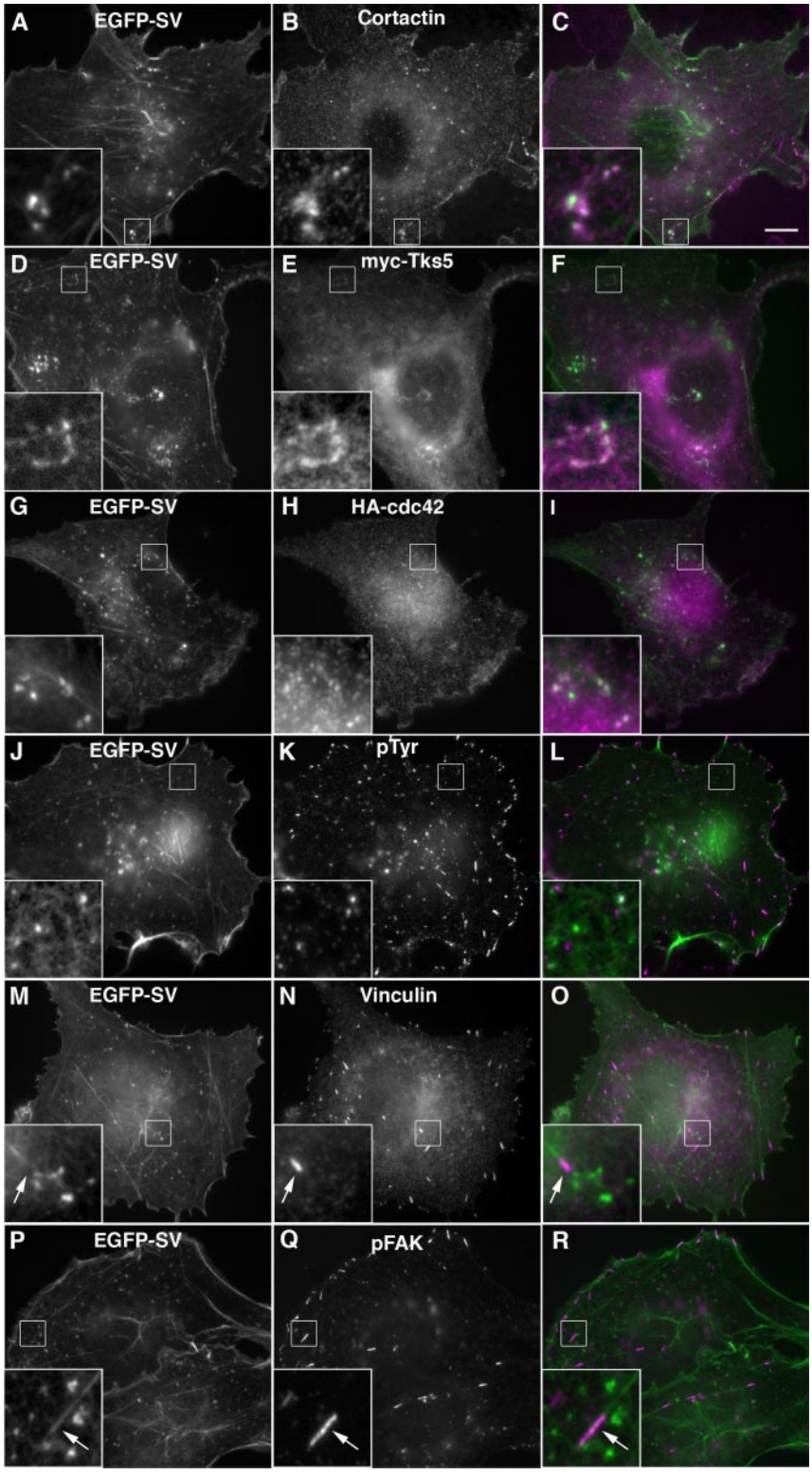

Figure 3. EGFP-SV punctae colocalize with cortactin and exogenous Tks5 and Cdc42 but not with phospho-FAK or vinculin. COS7 cells expressing EGFP-SV (A, D, G, J, M, and P) were stained with antibodies against endogenous cortactin (B), phosphotyrosine (pTyr; K), vinculin (N), or phosphorylated FAK (pFAK; Q) or with antibodies against tags on exogenously expressed Tks5 (E) or Cdc42 (H). EGFP-SV is green in the merged images (C, F, I, L, O, and R); other proteins are shown in magenta; overlap is white. Insets, fourfold enlargements of areas within boxes. Arrows denote focal adhesions. Bar, 10 μm.

A/ABP280 (Figure 5D-F) (Stendahl *et al.*, 1980). EGFP-SV induces a significant loss of lamellipodin from the cell periphery (Figure 5, A and B). By contrast, filamin remains at the cell periphery in COS7 cells expressing EGFP-SV, but the extent and intensity of the peripheral filamin signal seems reduced (Figure 5, D and E). Unlike the nearly perfect overlap seen with cortactin antibody (Figure 3, A–C), most EGFP-SV punctae lack lamellipodin and filamin (Figure 5, C and F, arrowheads), with only ~38 and ~35%, respectively, of the EGFP-SV punctae overlapping with signal from antibodies against these two proteins (Figure 5, C and F, arrows).

Cortactin Binds SV In Vitro. Due to the redistribution of cortactin upon EGFP-SV overexpression (Figure 4) and the

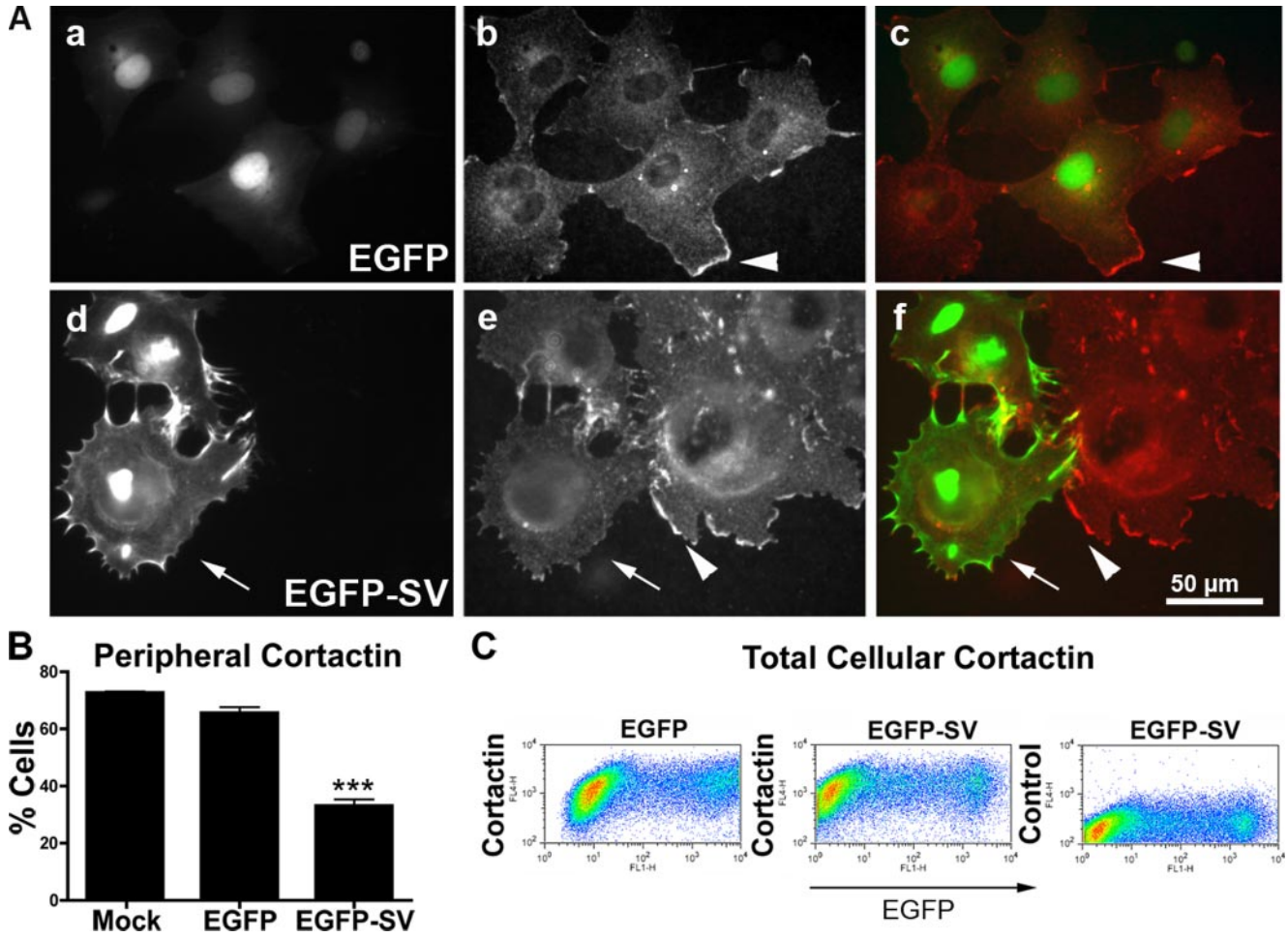

Figure 4. Expression of EGFP-SV leads to redistribution of cortactin. (A) COS7 cells expressing EGFP alone (a; green in c) or EGFP-SV (d; green in f) for 48 h were immunostained for endogenous cortactin (b and e; red in c and f). Cells were scored as containing (arrowheads) or lacking (arrows) peripheral cortactin. Bar, 50 μm. (B) Percentages of cells with continuous peripheral cortactin staining 48 h after mock transfection (Mock) or expression of EGFP alone (EGFP) or EGFP-SV (EGFP-SV). Means ± SD; ***$p < 0.0001$. (C) Two-color FACS analyses showing no change in the levels of total cellular cortactin caused by expression of EGFP or EGFP-SV in COS7 cells. Control, secondary antibody alone.

striking amount of colocalization of the two proteins (Figure 3, A–C), compared with the relatively weak overlap with lamellipodin and filamin (Figure 5, C and F), we investigated whether cortactin binds SV directly. GST or GST-tagged SV N-terminal fragments were mixed with His-cortactin(ΔSH3), and interacting proteins were co-sedimented with glutathione-Sepharose beads (Figure 6A). Even with significant His-cortactin(ΔSH3) input (Figure 6A, a and b, lanes 1), there was no detectable binding with GST or beads only (lanes 2 and 3). His-cortactin(ΔSH3) was pulled down with SV amino acids SV1-340 (lanes 4), SV570-830 (lanes 7), and SV340-830 (lanes 8). The lack of binding with SV171-340 (lanes 5) or SV340-570 (lanes 6) indicates likely cortactin binding sequences within SV1-171 and SV570-830.

Cortactin Increases the Numbers of EGFP-SV F-Actin Punctae. To see whether cortactin is necessary for the formation of EGFP-SV–induced F-actin punctae, we reduced cortactin levels by 74% of control-treated cells (Figure 6B, CON, lane 1) by using two different cortactin-specific siRNAs (*CT1* and *CT2*; lanes 2 and 3). Cortactin knockdown cells were transfected with plasmids encoding EGFP or EGFP-SV and scored for the number of F-actin punctae (Figure 6C). As in the absence of siRNA treatment (Figure 1), there is a significant difference between EGFP- and EGFP-SV–transfected cells treated with the control siRNA (***$p < 0.001$) (Figure 6C). Although cortactin knockdown has no significant effect on the numbers of F-actin punctae in EGFP-transfected cells, the reduction in cortactin levels inhibits ~50% of the increase in numbers induced by EGFP-SV (*$p < 0.05$). Therefore, the podosome and invadopodial protein cortactin contributes to the formation of EGFP-SV punctae.

Role of SV at Podosomes and Invadopodia

Endogenous SV Localizes to Src-induced Podosomes and Areas of Matrix Degradation in COS7 cells. To further examine the relationship between SV and podosomes/invadopodia, we localized endogenous SV in COS7 cells containing podosomes induced by constitutively active c-Src-Y527F (Figure 7). Each Src-induced podosome consists of a core of F-actin, cortactin, and other proteins surrounded by a ring of focal adhesion proteins (Linder and Aepfelbacher, 2003). Endogenous SV colocalizes extensively with F-actin and cortactin at the podosome cores (Figure 7, A and B) and less

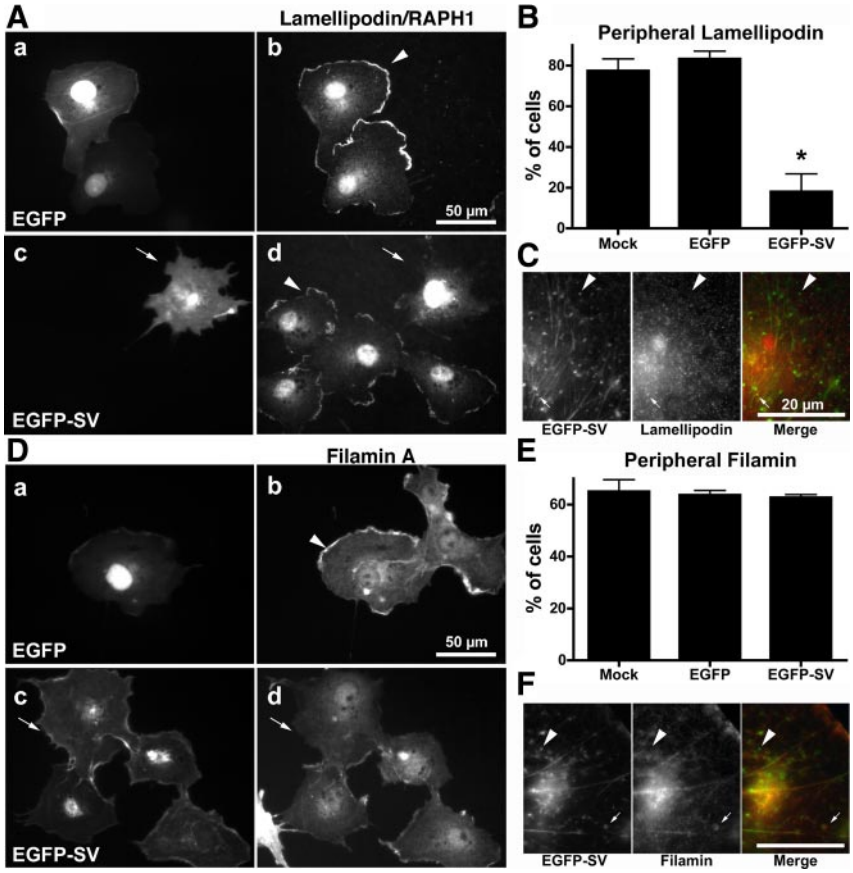

Figure 5. EGFP-SV redistributes lamellipodin/RAPH1/PREL1, but not filamin A, within 24 h. (A and D) COS7 cells expressing EGFP alone (a) or EGFP-SV (c) for 24 h were immunostained for endogenous lamellipodin (b and d in A) or filamin A (b and d in D). Cells were scored as containing (arrowheads) or lacking (arrows) peripherally localized protein. Bars, 50 μm. Percentages of cells with peripheral (B) lamellipodin or (E) filamin staining 24 h after mock transfection (Mock) or expression of EGFP alone (EGFP) or EGFP-SV (EGFP-SV). Means $\pm$ SD; *$p < 0.05$; $n = 2$ (B); $n = 3$ (E). Overlap (arrows) or lack of overlap (arrowheads) of EGFP-SV punctae with endogenous lamellipodin (C) and filamin (F). Bars, 20 μm.

well with α-actinin (Figure 7C), which associates with both the podosome core and ring (Linder and Aepfelbacher, 2003). Little overlap of SV with the focal adhesion proteins, phosphorylated FAK and vinculin, is observed in podosome rings (Figure 7, D and E). The overall SV staining pattern at podosome cores is generally more punctate than those of the other proteins (Figure 7, left, x-y inset), although foci of SV and cortactin show frequent overlaps (Figure 7B). Immunolocalization of SV shows a preferential exposure of the SV epitope at the apical ends of the podosomes, near the interface with the cytoplasm (Figure 7), regardless of whether SV is imaged with green (Figure 7) or red (Supplemental Figure S2A and S2B) fluorophores. However, colocalization of EGFP-SV and antibody-stained SV indicates that the N-terminal epitope recognized by the antibody is preferentially shielded near the base of the podosome cores (Supplemental Figure S2C). Thus, as has been reported for the transmembrane receptor CD44 (Chabadel *et al*., 2007), the peripheral membrane protein SV marks podosome cores. EGFP-SV also localizes to areas of matrix degradation in COS7 cells on fluorescently labeled gelatin although these cells do not efficiently degrade matrix (Supplemental Figure S3).

Many Tumor Cell Lines Contain Relatively High Levels of SV. To identify an invasive cell line in which we could examine SV function in matrix degradation and invasion, we screened a number of tumor cell lines for the presence of endogenous SV. Abundant levels of SV message have been reported in HeLa cervical adenocarcinoma, SW480 colorectal adenocarcinoma, and A549 lung carcinoma cells (Pope *et al*., 1998). In agreement with previous results (Pestonjamasp *et al*., 1997), we find that HeLa cells contain higher levels of endogenous SV than do untransformed cell lines (Supplemental Figure S4A, lanes 1–3). Several human prostate (LNCaP and C4-2, DU-145) (Stone *et al*., 1978; Thalmann *et al*., 1994) and breast (MCF10A1, MCF10AT1k.cl2, MCL10CA1h, MCF10ACA1a.cl1, and MDA-MB-231) (Tang *et al*., 2003) epithelial cell lines contain abundant endogenous SV (Supplemental Figure S4). The highest SV levels were seen in MDA-MB-231 metastatic breast carcinoma cells, which inherently form invadopodia on ECM substrates (Chen *et al*., 1994).

Endogenous SV Localizes to Invadopodia in MDA-MB-231 Cells. In MDA-MB-231 cells on gelatin, endogenous SV colocalizes with the large ventral accumulations of cortactin and F-actin characteristic of invadopodia (Figure 8A; Artym *et al*., 2006). In addition, mRFP-SV is found in proximity with ~45% of the vesicles or invadopodia that contain EGFP-MT1-MMP (Figure 8B), the membrane-bound MMP responsible for most matrix degradation in MDA-MB-231 cells (Artym *et al*., 2006). Endogenous SV also is concentrated at and within regions of matrix degradation, as identified by black areas in thin films of TRITC-labeled gelatin (Figure 8C). In XZ and YZ views, SV is seen both within and above the holes in the gelatin matrix created by invadopodia (Figure 8C, a–d). By contrast, little overlap is seen between EGFP-SV and the pY-100 phosphotyrosine antibody (Bowden *et al*., 2006; Supplemental Figure S5). Together, these data support an association between SV and invadopodia.

SV Overexpression Increases the Numbers of Matrix Degradation Sites Formed Per Cell. We tested whether SV affects ECM degradation in highly invasive MDA-MB-231 cells that

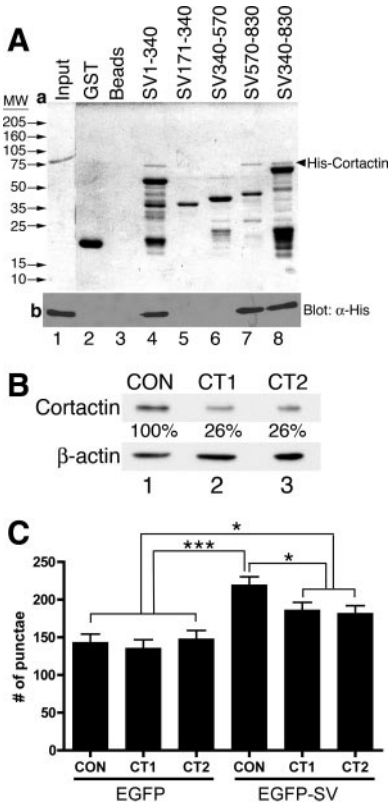

Figure 6. Cortactin binds SV in vitro and contributes to the formation of EGFP-SV–induced punctae in vivo. (A) His-cortactin(ΔSH3) (input, lane 1) was mixed with glutathione-Sepharose beads and the indicated GST fusion proteins (lanes 2 and 4–8) or with glutathione-Sepharose beads alone (lane 3) for 1 h. Beads were washed, pelleted, and heated in SDS sample buffer and interacting proteins were subjected to SDS-polyacrylamide gel electrophoresis and stained with Coomassie blue (a) or transferred to nitrocellulose and immunoblotted for the His tag (b) (n = 3). Arrowhead denotes His-cortactin(ΔSH3). Input lane (a) was digitally moved to match immunoblot (b). (B) Cortactin protein levels in COS7 cells 4 d after transfection with control siRNA (CON, lane 1) or cortactin siRNA (CT1, CT2, lanes 2, 3). β-actin was the loading control. Percent of cortactin remaining is shown under cortactin bands (n = 1). (C) Cortactin knockdown cells were transfected with plasmids encoding EGFP or EGFP-SV at day 3 of siRNA treatment, and F-actin punctae were visualized with phalloidin after an additional 24 h (n = 3). Statistically significant differences were determined by unpaired two-tailed Student's *t* tests and with the Student-Newman-Keuls multiple comparison test (*$p < 0.05$, ***$p < 0.001$).

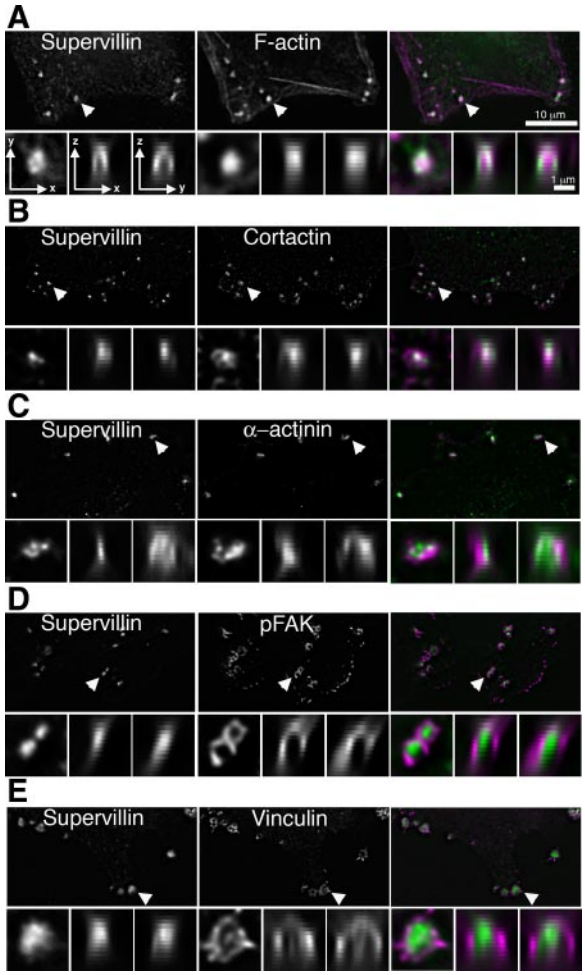

Figure 7. Endogenous supervillin localizes to the cores of Src-induced podosomes. COS7 cells were transfected with Y527F Src, immunostained for SV, and stained for F-actin with phalloidin (A) or with antibody against endogenous cortactin (B), α-actinin (C), pFAK (D), or vinculin (E) and visualized after deconvolution of images acquired with 0.2-μm Z-steps. F-actin and cortactin localize to podosome cores, α-actinin to cores + rings, and vinculin and pFAK to podosome rings (Linder and Aepfelbacher, 2003). Individual podosomes in the XY view (arrowheads) have been enlarged to the same scale as the XZ and YZ views. SV, green; other proteins magenta; and overlaps in white. Bars, 10 micrometers in main image, 1 μm in inset.

stably overexpress WT Src (MDA-MB-231/WT Src) (Myoui *et al*., 2003; Bowden *et al*., 2006). Transient overexpression of EGFP-SV to levels that were 4.9 ± 1.5 (mean ± SD; n = 3) times greater than endogenous SV levels doubled the average number of holes per cell in the fluorescent gelatin matrix (Figure 9B vs. A and C; and D). However, the percentage of cells that made holes did not differ significantly from controls (Figure 9E). Similar results are seen with MDA-MB-231 cells not transfected with c-Src (Supplemental Figure S6). This SV-promoted increase in the numbers of holes per cell corresponds to a 4.2-fold increase in the mean area of degraded matrix per cell (Supplemental Figure S7). These results are consistent with a SV-mediated increase in the numbers, efficiency, or dynamics of sites of ECM degradation.

SV Underexpression Decreases Matrix Degradation, Especially in the Cell Center. Conversely, reduction of endogenous SV levels reduces the apparent numbers of ECM-degrading sites (Figure 10). Each of two siRNAs reduces SV levels in MDA-MB-231/WT Src cells to ~30% of endogenous levels without adversely affecting the expression level of the related protein, gelsolin (Figure 10A, lanes 1–2 vs. lane 3). Although these reduced levels of SV do not affect the percentages of cells associated with degraded matrix (Figure 10B), the mean numbers of holes per cell (Figure 10C) and the percentages of cells with holes underneath the central region of the cell are decreased, compared with cells treated with a control siRNA (Figure 10D; and E, e vs. b). By contrast, matrix degradation in these assays is unaffected by down-regulation of gelsolin (Figure 10A, lane 4; and B–D), an SV family member involved in podosome assembly in osteoclasts and matrix invasion of MDA-MB-231 cells (Chellaiah *et al*., 2000; Van den Abbeele *et al*., 2007). Double knockdowns of SV and gelsolin (Figure 10A, lane 5) result in

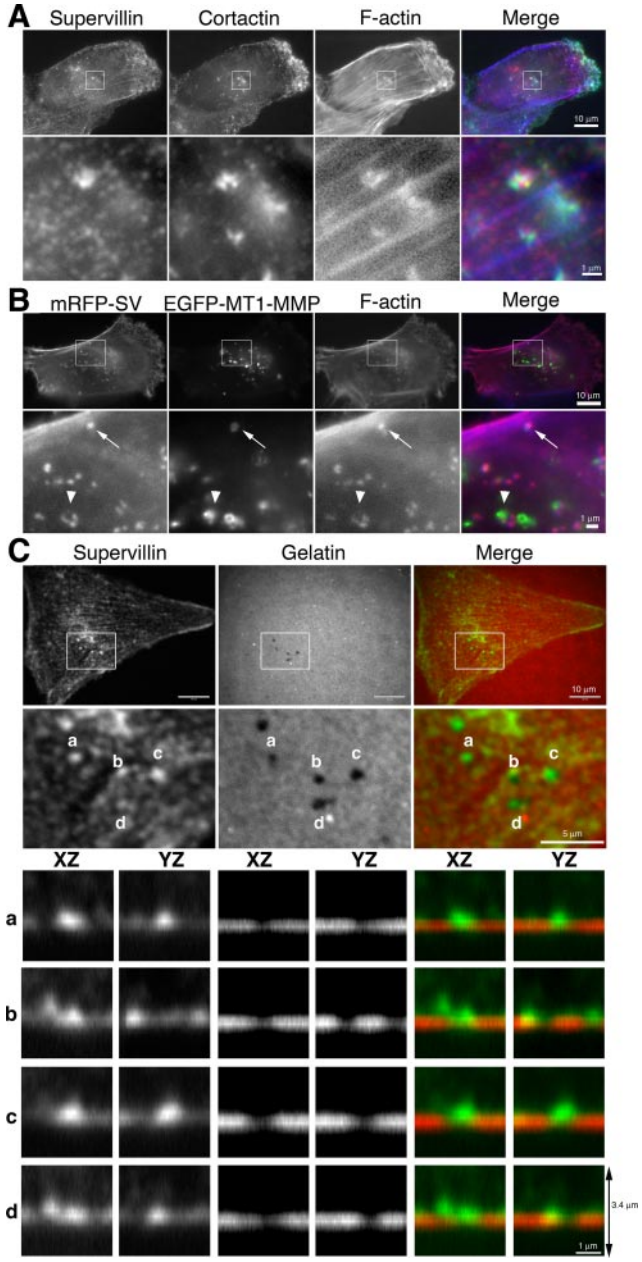

Figure 8. Supervillin localizes at and within MDA-MB-231 cell invadopodia. (A) MDA-MB-231 cells were plated on unlabeled gelatin for 3 h, fixed, and stained with antibodies (SV and cortactin) and/or phalloidin (F-actin) as noted, and then they were imaged by wide-field microscopy. Merges show supervillin (red), cortactin (green), and F-actin (blue). Bars, 10 μm (top row) and 1 μm (bottom row). (B) MDA-MB-231/WT Src cells were transfected with mRFP-SV and EGFP-MT1-MMP. Cells were plated on unlabeled gelatin-coated coverslips for 6 h, fixed, and stained with phalloidin (F-actin) and imaged by wide-field microscopy. Merges show mRFP-SV (red), EGFP-MT1-MMP (green), and F-actin (blue). Arrows indicate colocalization; arrowheads denote proximate localization. (C) MDA-MB-231 cells were plated on TRITC-labeled gelatin for 6 h, fixed, and stained with anti-SV antibodies, and then they were imaged by confocal microscopy as a Z-series with 0.2-μm steps. Merges show supervillin (green) and TRITC-gelatin (red). An XY view of such a cell is shown (top row). Areas inside the boxes were enlarged fourfold (second row). Eightfold enlargements of XZ and YZ views corresponding to a, b, c, and d are shown below XY views. Bars, 10 μm (top row), 5 μm (second row), and 1 μm (bottom row).

the same number of total holes per cell as observed for controls (Figure 10C) and are not significantly more effective than knockdown of SV alone in decreasing the presence of central holes (Figure 10D). However, the locations of the holes in the matrix for the SV/gelsolin double knockdown tended to be shifted away from the cell centers toward the cell edges, as was also observed for knockdown of SV alone (Figure 10Eh). Thus, SV apparently affects both the numbers and locations of the holes in the fluorescent matrix.

SV Knockdown Does Not Decrease Ventral F-Actin Punctae. Although SV can increase F-actin bundling in vitro and in vivo (Wulfkuhle *et al*., 1999; Chen *et al*., 2003), SV probably is not required for the formation of ventral F-actin structures (Figure 10E). MDA-MB-231/WT Src cells with reduced levels of SV and significantly reduced sites of matrix degradation (Figure 10E, e, h vs. b) still contain apparently normal levels of F-actin structures within the ventral focal plane (Figure 10E, d, g vs. a). In addition, COS7 cells expressing constitutively active c-Src-Y527F form similar numbers of podosomes, regardless of whether their SV levels are normal or have been reduced to 20 $\pm$ 5% of endogenous levels (Supplemental Figure S8). The normal-looking appearance of the ventral F-actin structures in SV knockdown cells, coupled with the reduced numbers of associated ECM holes in MDA-MB-231/WT Src cells, suggest a defect in invadopodial function.

SV Knockdown Reduces Invasion, but Only in the Context of Reduced Levels of Gelsolin. As a direct assay for the roles of SV and gelsolin in invasion, we measured the effects of single and double SV and gelsolin knockdowns on the ability of MDA-MB-231/WT Src cells to invade Matrigel-coated transwell filters (Figure 11). Invasion indices are normalized to eliminate effects of changes in cell motility although no statistically significant differences are apparent in the rates of cell transmigration across uncoated filters at this long time point (data not shown). Knockdown of SV alone shows an upward trend in invasion index (Figure 11), and reduction of gelsolin alone shows a downward trend that compares favorably with previously published results (Van den Abbeele *et al*., 2007). However, assay-to-assay variances preclude statistical significance for single knockdowns of either SV or gelsolin. By contrast, simultaneously reducing SV and gelsolin significantly decreases the ability of MDA-MB-231 cells to invade Matrigel-coated filters.

DISCUSSION

We show here that SV reorganizes the cortical actin cytoskeleton, stimulating the formation or redistribution of dynamic basal punctae containing F-actin, cortactin, and other podosome/invadopodia proteins while decreasing the extents of cortactin and lamellipodin at the cell periphery. SV and cortactin bind directly in vitro and cooperate to redistribute F-actin in vivo. We also show that SV is a core component of Src-induced podosomes and invadopodia and that SV contributes to ECM degradation and Matrigel invasion by Src-expressing MDA-MB-231 breast carcinomas. These results are consistent with the report that the gene encoding SV, SVIL, is among the predisposing factors for nonBRCA1/2 (BRCAx) breast cancer (Hedenfalk *et al*., 2003).

One possible mechanism of SV action is alteration of signaling pathways upstream of cytoskeletal remodeling. The earliest change that we see in lamellipodial architecture in cells expressing EGFP-SV is the loss of peripheral lamellipodin (Figure 5). Lamellipodin regulates actin polymeriza-

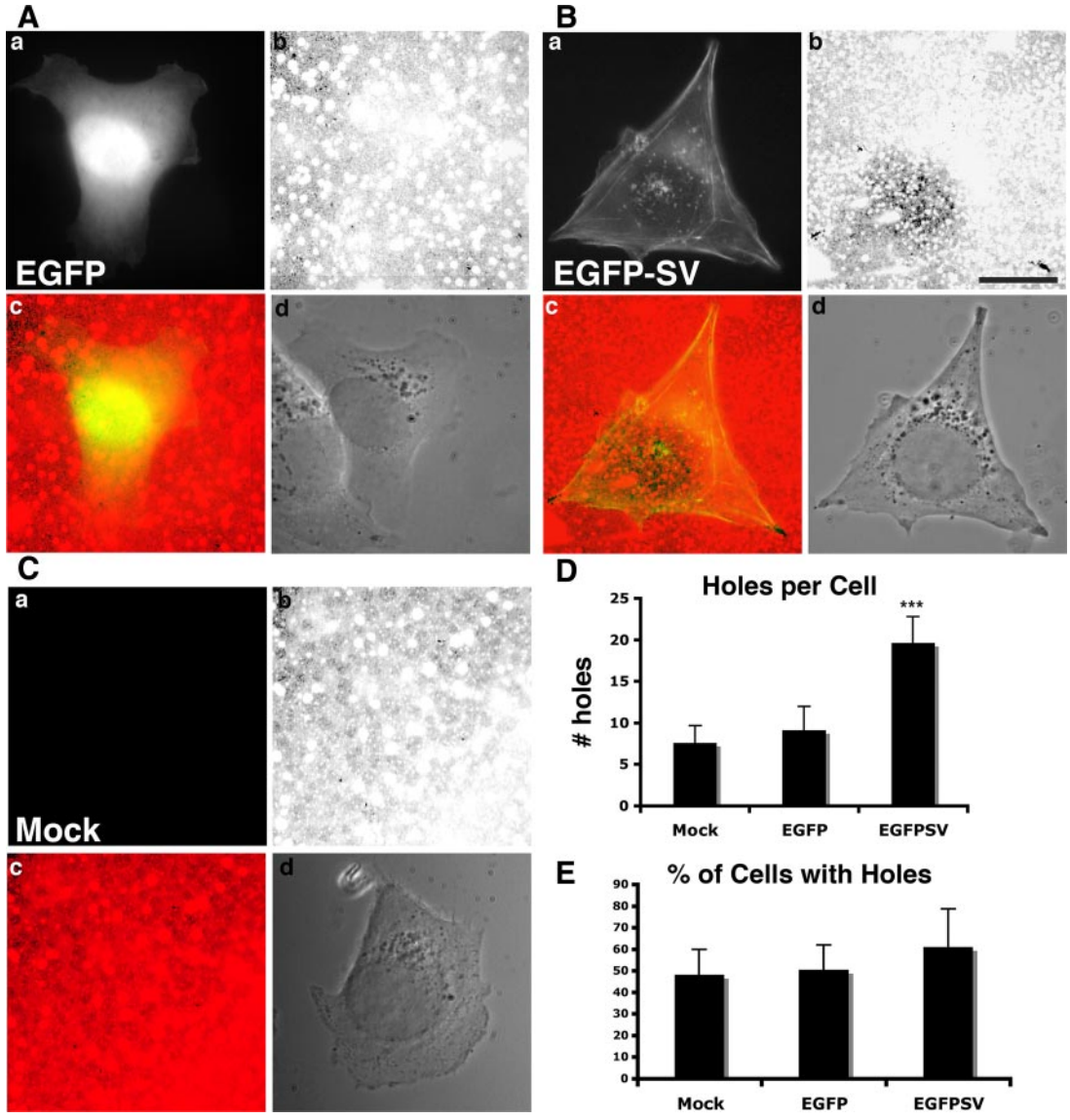

Figure 9. Overexpression of EGFP-SV increases the number of matrix holes formed per cell. MDA-MB-231/WT Src cells were transfected with either EGFP alone (A) or EGFP-SV (B) or they were mock transfected (C). Cells were plated on TRITC-labeled gelatin for 6 h before visualization by green (a) and red (b) fluorescence and phase contrast (d); merged green and red images also are shown (c). Bar, 20 μm. (D) The numbers of holes in the red gelatin matrix (representative of invadopodia) per cell were counted. EGFP-SV cells had a significant (***$p < 0.001$; $n = 8$) increase in the number of associated holes per cell. (E) The percentage of cells with some matrix degradation was not significantly different among the three conditions.

tion mediated by Ena/VASP family proteins downstream of Ras activation (Krause *et al*., 2004; Jenzora *et al*., 2005). The lack of extensive overlap between lamellipodin and SV in punctae argues against a direct interaction between these two proteins. However, an indirect negative effect of SV on lamellipodial organization at the cell periphery could lead to the loss of broad arcs of peripheral F-actin, cortactin, and lamellipodin that we observe (Figures 4 and 5).

A second possibility is that SV-induced punctae may represent podosome/invadopodia "building blocks" associated with vesicles and/or molecular motors at various stages of assembly or intracellular transit. SV may help recruit cortactin and F-actin to intracellular membranes. Because SV, cortactin, and filamin all bind F-actin, the lack of filamin recruitment to punctae argues for a selective association with cortactin. A membrane-based mechanism for SV is likely based on its intracellular distribution and fractionation behavior (Pestonjamasp *et al*., 1997; Wulfkuhle *et al*., 1999; Nebl *et al*., 2002; Oh *et al*., 2003; Takizawa *et al*., 2006). The dot-like appearances of many EGFP-SV punctae (Figures 1 and 3) and XY views of endogenous SV at podosomes (Figure 7) are reminiscent of vesicles, as are the circular profiles that are occasionally apparent for larger structures associated with EGFP-SV (Figure 2 and Supplemental Video 1). EGFP-SV/F-actin/cortactin punctae also resemble cortactin structures described as occurring before actin recruitment in phorbol ester-induced podosomes (Webb *et al*., 2006a) or originating at lamellipodia and moving in association with endosomes (Kaksonen *et al*., 2000; Boguslavsky *et al*., 2007; Lladó *et al*., 2008). Although we did not detect consistent directional trafficking of SV punctae from the cell periphery to the basolateral cell surface, subtle effects on vesicle trafficking or

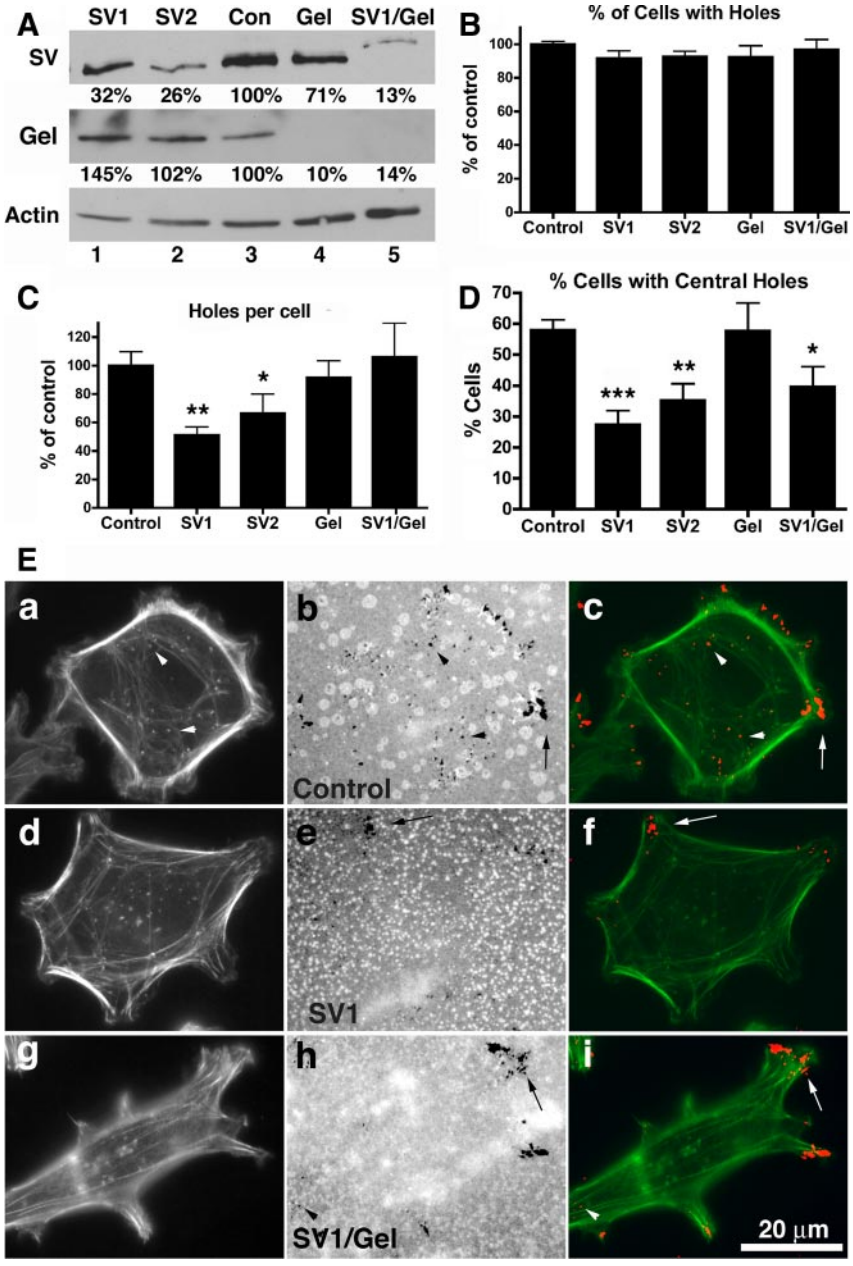

Figure 10. Underexpression of endogenous SV decreases the numbers of matrix holes per cell, especially under the center of the cell. MDA-MB-231/WT Src cells were transfected with either control siRNA (Con) or siRNAs targeting SV (SV1 and SV2), the related protein, gelsolin (Gel), or both SV and gelsolin (SV1/Gel). These cells were analyzed for protein levels by immunoblotting (A); the percentages of cells associated with at least one area of degraded matrix (hole), relative to control-treated cells (B); the mean numbers of holes per cell, relative to control-treated cells (C); and the percentages of cells with holes underneath the cell center (D). The percentages in A denote the mean levels (n = 4) of SV and gelsolin, relative to control-treated cells, after normalization to the β-actin loading control. (B–D) Means ± SD; n = 6. Asterisks in C and D denote significant differences (***$p < 0.001$, **$p < 0.01$, and *$p < 0.05$) from controls in unpaired t tests. (E) Representative micrographs of cells treated with control siRNA (a–c), SV1 siRNA (d–f), or both SV1 and gelsolin (SV1/Gel) siRNAs (g–i) and stained for F-actin (a, d, and g) or sites of matrix degradation (b, e, and h). For merged images (c, f, and i), holes in the matrix were visualized as red spots by pseudocoloring the images in b, e, and h after inverting and thresholding their luminosities. Note the sites of matrix degradation at the cell periphery (arrows) and underneath the cell center (arrowheads). Overlaps are yellow or orange. Bar, 20 μm.

on cortactin recruitment to transport vesicles could lead to the observed shift in cortactin and F-actin distribution over time.

A selective effect of SV on basolateral targeting of cortactin and MMPs would be consistent both with the observed effects of SV knockdown on sites of matrix degradation under the cell center (Figure 10) and with the role of cortactin in MMP trafficking and matrix degradation (Bowden *et al*., 1999; Artym *et al*., 2006; Clark *et al*., 2007; Clark and Weaver, 2008). Cortactin recruitment to the ventral cell surface occurs in stages, mediated by at least three convergent regulatory signals (Artym *et al*., 2006; Webb *et al*., 2006a; Ayala *et al*., 2008). Activating mechanisms include cortactin phosphorylation by ERK1/2, Src family kinases, and PAK (Webb *et al*., 2006b; Tehrani *et al*., 2007; Ayala *et al*., 2008). In this context, we note that an isoform of SV is involved in stimulus-mediated activation of ERK1/2 in smooth muscle (Gangopadhyay *et al*., 2004) and that SV binds directly to and regulates myosin II (Takizawa *et al*., 2007), which directly affects exocytosis in a number of cell types (Togo and Steinhardt, 2004). The sequential regulated recruitment of MMPs and other proteins to invadopodia suggests that subsequent matrix degradation is a dynamic multistep process (Artym *et al*., 2006; Clark *et al*., 2007; Block *et al*., 2008). Our SV knockdown results (Figure 10) are consistent with SV-mediated increases in cortactin activation, enhanced cortactin- or myosin II-mediated MMP secretion, and/or elevation of the rate of invadopodia turnover.

The decreased matrix degradation generated by knockdowns of either SV, cortactin, or Tks5 and the colocalization of all three proteins at SV-induced punctae suggests functional cooperation (Seals *et al*., 2005; Artym *et al*., 2006; Clark *et al*., 2007; Webb *et al*., 2007; Ayala *et al*., 2008; Clark and Weaver, 2008). Participation in a common pathway is fur-

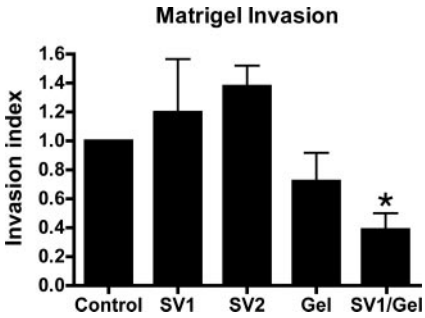

Figure 11. Invasion indices are decreased in cells depleted of both SV and gelsolin. MDA-MB-231/WT Src cells were treated with either control siRNA (Control) or with siRNAs targeting either SV (SV1 and SV2), gelsolin (Gel), or both proteins (SV1/Gel) and assayed for invasion through Matrigel-coated filters. Cells depleted in both SV and gelsolin were significantly less invasive than controls, based on unpaired *t* tests (*$p < 0.05$; $n = 3$).

ther supported by the interaction of SV with cortactin and by the decreased formation of EGFP-SV induced F-actin punctae in cortactin knockdown cells (Figure 6). Thus, these proteins may cooperate in signaling and/or cytoskeletal organization during invadopodia formation. However, F-actin structures form at Src-induced podosomes and at the ventral surfaces of MDA-MB-231 cells after SV knockdown, arguing for SV-independent effects during initial cytoskeletal assembly.

Our results support the hypothesis that SV promotes the loss of large central focal adhesions (Takizawa *et al*., 2006) by increasing local matrix degradation. The effects of SV overexpression on large focal adhesions and on ECM degradation both represent a gain of function because reduction of endogenous SV exhibits the opposite phenotype (Takizawa *et al*., 2006; Figures 9 and 10). SV targeting to focal adhesions by binding to TRIP6 (Takizawa *et al*., 2006) could lead to a loss of underlying matrix, causing detachment of integrins and thereby inducing focal adhesion disassembly.

Surprisingly, we find that the outcomes of gelatin degradation experiments with SV and gelsolin (Figure 10) do not predict the results of Matrigel invasion assays (Figure 11). This might be due to the fine line between degrading enough ECM for transmigration versus destroying too much underlying matrix for the adhesion necessary for movement. These observations are consistent with the report that down-regulation of MT1-MMP can actually increase invasion (Partridge *et al*., 2007). The long time courses of invasion assays also allow for other mechanisms, such as alterations in cell motility or proliferation in response to the growth factors that can be released from Matrigel (Kleinman and Martin, 2005). Commonalities in signaling mechanisms could explain the functional redundancy between SV and gelsolin during Matrigel invasion, especially if SV can recruit actin to membranes enriched in phosphatidylinositol bisphosphate, as suggested by the similarities between SV and gelsolin sequences involved in this process (Hartwig *et al*., 1989; Mere *et al*., 2005). Gelsolin and CapG, another member of the villin/gelsolin family, also synergize with each other during matrix invasion and have each been implicated in multiple stages of tumorigenesis (Dong *et al*., 1999; Lee *et al*., 1999; Silacci *et al*., 2004; Watari *et al*., 2006; Kim *et al*., 2007; Van den Abbeele *et al*., 2007; Nomura *et al*., 2008). We conclude that SV plays a nonredundant role in ECM degradation by MDA-MB-231 breast carcinoma cells and has a function overlapping that of gelsolin during invasion, both of which are important facets of tumor cell migration and metastasis.

ACKNOWLEDGMENTS

We thank Dr. Paul Furcinitti (University of Massachusetts Medical School Biomedical Imaging Facility) for assistance in acquiring confocal images and Sneha Arjun (Worcester Polytechnic Institute) and Shruti Basil (College of the Holy Cross) for assistance with blinded scoring of images. We thank Dr. Frank Gertler for anti-lamellipodin antibody and Drs. Susette Mueller and Toshiyuki Yoneda for MDA-MB-231 cell lines. We also thank Drs. Greenfield Sluder, Lucia Languino, K. C. Balaji, and Arthur Mercurio for gifts of immortalized and transformed cells used for immunoblots and Drs. Sara A Courtneidge, Kozo Kaibuchi, Alan Mak, Maria Montoya, and Harold Varmus for plasmids. In addition, we gratefully acknowledge Drs. Stefan Linder and Susette Mueller for valuable experimental suggestions and critical comments on the manuscript. This project was supported by National Institutes of Health grant GM-33048 and benefited from the Department of Defense Breast Cancer Program award W81XWH-0410642.

REFERENCES

Ammer, A. G., and Weed, S. A. (2008). Cortactin branches out: roles in regulating protrusive actin dynamics. Cell Motil. Cytoskeleton *65*, 687–707.

Archer, S. K., Claudianos, C., and Campbell, H. D. (2005). Evolution of the gelsolin family of actin-binding proteins as novel transcriptional coactivators. Bioessays *27*, 388–396.

Artym, V. V., Zhang, Y., Seillier-Moiseiwitsch, F., Yamada, K. M., and Mueller, S. C. (2006). Dynamic interactions of cortactin and membrane type 1 matrix metalloproteinase at invadopodia: defining the stages of invadopodia formation and function. Cancer Res *66*, 3034–3043.

Ayala, I., Baldassarre, M., Giacchetti, G., Caldieri, G., Tete, S., Luini, A., and Buccione, R. (2008). Multiple regulatory inputs converge on cortactin to control invadopodia biogenesis and extracellular matrix degradation. J. Cell Sci. *121*, 369–378.

Bai, C. Y., Ohsugi, M., Abe, Y., and Yamamoto, T. (2007). ZRP-1 controls Rho GTPase-mediated actin reorganization by localizing at cell-matrix and cell-cell adhesions. J. Cell Sci. *120*, 2828–2837.

Baldassarre, M., Pompeo, A., Beznoussenko, G., Castaldi, C., Cortellino, S., McNiven, M. A., Luini, A., and Buccione, R. (2003). Dynamin participates in focal extracellular matrix degradation by invasive cells. Mol. Biol. Cell *14*, 1074–1084.

Benesch, S., Lommel, S., Steffen, A., Stradal, T. E., Scaplehorn, N., Way, M., Wehland, J., and Rottner, K. (2002). Phosphatidylinositol 4,5-biphosphate (PIP2)-induced vesicle movement depends on N-WASP and involves Nck, WIP, and Grb2. J. Biol. Chem. *277*, 37771–37776.

Block, M. R., Badowski, C., Millon-Fremillon, A., Bouvard, D., Bouin, A. P., Faurobert, E., Gerber-Scokaert, D., Planus, E., and Albiges-Rizo, C. (2008). Podosome-type adhesions and focal adhesions, so alike yet so different. Eur. J. Cell Biol. *87*, 491–506.

Boguslavsky, S., Grosheva, I., Landau, E., Shtutman, M., Cohen, M., Arnold, K., Feinstein, E., Geiger, B., and Bershadsky, A. (2007). p120 catenin regulates lamellipodial dynamics and cell adhesion in cooperation with cortactin. Proc. Natl. Acad. Sci. USA *104*, 10882–10887.

Bowden, E. T., Barth, M., Thomas, D., Glazer, R. I., and Mueller, S. C. (1999). An invasion-related complex of cortactin, paxillin and PKCmu associates with invadopodia at sites of extracellular matrix degradation. Oncogene *18*, 4440–4449.

Bowden, E. T., Coopman, P. J., and Mueller, S. C. (2001). Invadopodia: unique methods for measurement of extracellular matrix degradation *in vitro*. Methods Cell Biol. *63*, 613–627.

Bowden, E. T., Onikoyi, E., Slack, R., Myoui, A., Yoneda, T., Yamada, K. M., and Mueller, S. C. (2006). Co-localization of cortactin and phosphotyrosine identifies active invadopodia in human breast cancer cells. Exp. Cell Res. *312*, 1240–1253.

Bravo-Cordero, J. J., Marrero-Diaz, R., Megias, D., Genis, L., Garcia-Grande, A., Garcia, M. A., Arroyo, A. G., and Montoya, M. C. (2007). MT1-MMP proinvasive activity is regulated by a novel Rab8-dependent exocytic pathway. EMBO J. *26*, 1499–1510.

Broussard, J. A., Webb, D. J., and Kaverina, I. (2008). Asymmetric focal adhesion disassembly in motile cells. Curr. Opin. Cell Biol. *20*, 85–90.

Buday, L., and Downward, J. (2007). Roles of cortactin in tumor pathogenesis. Biochim. Biophys. Acta *1775*, 263–273.

Chabadel, A., Banon-Rodriguez, I., Cluet, D., Rudkin, B. B., Wehrle-Haller, B., Genot, E., Jurdic, P., Anton, I. M., and Saltel, F. (2007). CD44 and beta3 integrin organize two functionally distinct actin-based domains in osteoclasts. Mol. Biol. Cell *18*, 4899–4910.

Chellaiah, M., Kizer, N., Silva, M., Alvarez, U., Kwiatkowski, D., and Hruska, K. A. (2000). Gelsolin deficiency blocks podosome assembly and produces increased bone mass and strength. J. Cell Biol. *148*, 665–678.

Chen, W. T., *et al*. (1994). Membrane proteases as potential diagnostic and therapeutic targets for breast malignancy. Breast Cancer Res Treat *31*, 217–226.

Chen, W. T., and Wang, J. Y. (1999). Specialized surface protrusions of invasive cells, invadopodia and lamellipodia, have differential MT1-MMP, MMP-2, and TIMP-2 localization. Ann. N Y Acad. Sci. *878*, 361–371.

Chen, Y., Takizawa, N., Crowley, J. L., Oh, S. W., Gatto, C. L., Kambara, T., Sato, O., Li, X., Ikebe, M., and Luna, E. J. (2003). F-actin and myosin II binding domains in supervillin. J. Biol. Chem. *278*, 46094–46106.

Clark, E. S., and Weaver, A. M. (2008). A new role for cortactin in invadopodia: regulation of protease secretion. Eur. J. Cell Biol. *87*, 581–590.

Clark, E. S., Whigham, A. S., Yarbrough, W. G., and Weaver, A. M. (2007). Cortactin is an essential regulator of matrix metalloproteinase secretion and extracellular matrix degradation in invadopodia. Cancer Res. *67*, 4227–4235.

Condeelis, J., Singer, R. H., and Segall, J. E. (2005). The great escape: when cancer cells hijack the genes for chemotaxis and motility. Annu. Rev. Cell Dev. Biol. *21*, 695–718.

Courtneidge, S. A., Azucena, E. F., Pass, I., Seals, D. F., and Tesfay, L. (2005). The SRC substrate Tks5, podosomes (invadopodia), and cancer cell invasion. Cold Spring Harb. Symp. Quant. Biol. *70*, 167–171.

De Corte, V., Bruyneel, E., Boucherie, C., Mareel, M., Vandekerckhove, J., and Gettemans, J. (2002). Gelsolin-induced epithelial cell invasion is dependent on Ras-Rac signaling. EMBO J. *21*, 6781–6790.

Destaing, O., Saltel, F., Geminard, J. C., Jurdic, P., and Bard, F. (2003). Podosomes display actin turnover and dynamic self-organization in osteoclasts expressing actin-green fluorescent protein. Mol. Biol. Cell *14*, 407–416.

Dong, Y., Asch, H. L., Medina, D., Ip, C., Ip, M., Guzman, R., and Asch, B. B. (1999). Concurrent deregulation of gelsolin and cyclin D1 in the majority of human and rodent breast cancers. Int. J. Cancer *81*, 930–938.

Evans, J. G., and Matsudaira, P. (2006). Structure and dynamics of macrophage podosomes. Eur. J. Cell Biol. *85*, 145–149.

Furmaniak-Kazmierczak, E., Crawley, S. W., Carter, R. L., Maurice, D. H., and Cote, G. P. (2007). Formation of extracellular matrix-digesting invadopodia by primary aortic smooth muscle cells. Circ. Res. *100*, 1328–1336.

Galvez, B. G., Matias-Roman, S., Yanez-Mo, M., Sanchez-Madrid, F., and Arroyo, A. G. (2002). ECM regulates MT1-MMP localization with beta1 or alphavbeta3 integrins at distinct cell compartments modulating its internalization and activity on human endothelial cells. J. Cell Biol. *159*, 509–521.

Gangopadhyay, S. S., Takizawa, N., Gallant, C., Barber, A. L., Je, H. D., Smith, T. C., Luna, E. J., and Morgan, K. G. (2004). Smooth muscle archvillin: a novel regulator of signaling and contractility in vascular smooth muscle. J. Cell Sci. *117*, 5043–5057.

Gavazzi, I., Nermut, M. V., and Marchisio, P. C. (1989). Ultrastructure and gold-immunolabelling of cell-substratum adhesions (podosomes) in RSV-transformed BHK cells. J. Cell Sci. *94*, 85–99.

Gimona, M., Buccione, R., Courtneidge, S. A., and Linder, S. (2008). Assembly and biological role of podosomes and invadopodia. Curr. Opin. Cell Biol. *20*, 235–241.

Gimona, M., Kaverina, I., Resch, G. P., Vignal, E., and Burgstaller, G. (2003). Calponin repeats regulate actin filament stability and formation of podosomes in smooth muscle cells. Mol. Biol. Cell *14*, 2482–2491.

Hartwig, J. H., Chambers, K. A., and Stossel, T. P. (1989). Association of gelsolin with actin filaments and cell membranes of macrophages and platelets. J. Cell Biol. *108*, 467–479.

Hedenfalk, I., *et al*. (2003). Molecular classification of familial non-BRCA1/BRCA2 breast cancer. Proc. Natl. Acad. Sci. USA *100*, 2532–2537.

Ingley, E. (2008). Src family kinases: regulation of their activities, levels and identification of new pathways. Biochim. Biophys. Acta *1784*, 56–65.

Jenzora, A., Behrendt, B., Small, J. V., Wehland, J., and Stradal, T. E. (2005). PREL1 provides a link from Ras signalling to the actin cytoskeleton via Ena/VASP proteins. FEBS Lett. *579*, 455–463.

Kaksonen, M., Peng, H. B., and Rauvala, H. (2000). Association of cortactin with dynamic actin in lamellipodia and on endosomal vesicles. J. Cell Sci. *113*, 4421–4426.

Khurana, S., and George, S. P. (2008). Regulation of cell structure and function by actin-binding proteins: villin's perspective. FEBS Lett. *582*, 2128–2139.

Kim, C. S., Furuya, F., Ying, H., Kato, Y., Hanover, J. A., and Cheng, S. Y. (2007). Gelsolin: a novel thyroid hormone receptor-beta interacting protein that modulates tumor progression in a mouse model of follicular thyroid cancer. Endocrinology *148*, 1306–1312.

Kleinman, H. K., and Martin, G. R. (2005). Matrigel: basement membrane matrix with biological activity. Semin. Cancer Biol. *15*, 378–386.

Kowalczyk, A. P., Bornslaeger, E. A., Borgwardt, J. E., Palka, H. L., Dhaliwal, A. S., Corcoran, C. M., Denning, M. F., and Green, K. J. (1997). The amino-terminal domain of desmoplakin binds to plakoglobin and clusters desmosomal cadherin-plakoglobin complexes. J. Cell Biol. *139*, 773–784.

Krause, M., *et al*. (2004). Lamellipodin, an Ena/VASP ligand, is implicated in the regulation of lamellipodial dynamics. Dev. Cell *7*, 571–583.

Laemmli, U. K. (1970). Cleavage of structural proteins during the assembly of the head of bacteriophage T4. Nature *227*, 680–685.

Lai, Y. J., Chen, C. S., Lin, W. C., and Lin, F. T. (2005). c-Src-mediated phosphorylation of TRIP6 regulates its function in lysophosphatidic acid-induced cell migration. Mol. Cell. Biol. *25*, 5859–5868.

Lai, Y. J., Lin, W. C., and Lin, F. T. (2007). PTPL1/FAP-1 negatively regulates TRIP6 function in lysophosphatidic acid-induced cell migration. J. Biol. Chem. *282*, 24381–24387.

Lee, H. K., Driscoll, D., Asch, H., Asch, B., and Zhang, P. J. (1999). Down-regulated gelsolin expression in hyperplastic and neoplastic lesions of the prostate. Prostate *40*, 14–19.

Linder, S. (2007). The matrix corroded: podosomes and invadopodia in extracellular matrix degradation. Trends Cell Biol. *17*, 107–117.

Linder, S., and Aepfelbacher, M. (2003). Podosomes: adhesion hot-spots of invasive cells. Trends Cell Biol. *13*, 376–385.

Lladó, A., Timpson, P., Vila de Muga, S., Moreto, J., Pol, A., Grewal, T., Daly, R. J., Enrich, C., and Tebar, F. (2008). Protein Kinase C{delta} and calmodulin regulate epidermal growth factor receptor recycling from early endosomes through Arp2/3 complex and cortactin. Mol. Biol. Cell *19*, 17–29.

Lo, S. H. (2006). Focal adhesions: what's new inside. Dev. Biol. *294*, 280–291.

Lock, P., Abram, C. L., Gibson, T., and Courtneidge, S. A. (1998). A new method for isolating tyrosine kinase substrates used to identify fish, an SH3 and PX domain-containing protein, and Src substrate. EMBO J. *17*, 4346–4357.

Machesky, L., Jurdic, P., and Hinz, B. (2008). Grab, stick, pull and digest: the functional diversity of actin-associated matrix-adhesion structures. Workshop on Invadopodia, Podosomes and Focal Adhesions in Tissue Invasion. EMBO Rep. *9*, 139–143.

MacLennan, A. J., Orringer, M. B., and Beer, D. G. (1999). Identification of intestinal-type Barrett's metaplasia by using the intestine-specific protein villin and esophageal brush cytology. Mol. Carcinog. *24*, 137–143.

Mareel, M., and Leroy, A. (2003). Clinical, cellular, and molecular aspects of cancer invasion. Physiol. Rev. *83*, 337–376.

Mere, J., Chahinian, A., Maciver, S. K., Fattoum, A., Bettache, N., Benyamin, Y., and Roustan, C. (2005). Gelsolin binds to polyphosphoinositide-free lipid vesicles and simultaneously to actin microfilaments. Biochem. J. *386*, 47–56.

Mizushima, S., and Nagata, S. (1990). pEF-BOS, a powerful mammalian expression vector. Nucleic Acids Res. *18*, 5322.

Myoui, A., Nishimura, R., Williams, P. J., Hiraga, T., Tamura, D., Michigami, T., Mundy, G. R., and Yoneda, T. (2003). C-SRC tyrosine kinase activity is associated with tumor colonization in bone and lung in an animal model of human breast cancer metastasis. Cancer Res. *63*, 5028–5033.

Nakahara, H., Otani, T., Sasaki, T., Miura, Y., Takai, Y., and Kogo, M. (2003). Involvement of Cdc42 and Rac small G proteins in invadopodia formation of RPMI7951 cells. Genes Cells *8*, 1019–1027.

Nebl, T., Pestonjamasp, K. N., Leszyk, J. D., Crowley, J. L., Oh, S. W., and Luna, E. J. (2002). Proteomic analysis of a detergent-resistant membrane skeleton from neutrophil plasma membranes. J. Biol. Chem. *277*, 43399–43409.

Nitsch, L., Gionti, E., Cancedda, R., and Marchisio, P. C. (1989). The podosomes of Rous sarcoma virus transformed chondrocytes show a peculiar ultrastructural organization. Cell Biol. Int. Rep. *13*, 919–926.

Nomura, H., *et al*. (2008). Clinical significance of gelsolin-like actin-capping protein expression in oral carcinogenesis: an immunohistochemical study of premalignant and malignant lesions of the oral cavity. BMC Cancer *8*, 39.

Ochoa, G. C., *et al*. (2000). A functional link between dynamin and the actin cytoskeleton at podosomes. J. Cell Biol. *150*, 377–389.

Oh, S. W., Pope, R. K., Smith, K. P., Crowley, J. L., Nebl, T., Lawrence, J. B., and Luna, E. J. (2003). Archvillin, a muscle-specific isoform of supervillin, is an early expressed component of the costameric membrane skeleton. J. Cell Sci. *116*, 2261–2275.

Paluch, E., van der Gucht, J., Joanny, J. F., and Sykes, C. (2006). Deformations in actin comets from rocketing beads. Biophys. J. *91*, 3113–3122.

Partridge, J. J., Madsen, M. A., Ardi, V. C., Papagiannakopoulos, T., Kupriyanova, T. A., Quigley, J. P., and Deryugina, E. I. (2007). Functional analysis of matrix metalloproteinases and tissue inhibitors of metalloproteinases differentially expressed by variants of human HT-1080 fibrosarcoma exhibiting high and low levels of intravasation and metastasis. J. Biol. Chem. *282*, 35964–35977.

Perrin, B. J., Amann, K. J., and Huttenlocher, A. (2006). Proteolysis of cortactin by calpain regulates membrane protrusion during cell migration. Mol. Biol. Cell *17*, 239–250.

Pestonjamasp, K. N., Pope, R. K., Wulfkuhle, J. D., and Luna, E. J. (1997). Supervillin (p205): a novel membrane-associated, F-actin-binding protein in the villin/gelsolin superfamily. J. Cell Biol. *139*, 1255–1269.

Pope, R. K., Pestonjamasp, K. N., Smith, K. P., Wulfkuhle, J. D., Strassel, C. P., Lawrence, J. B., and Luna, E. J. (1998). Cloning, characterization, and chromosomal localization of human supervillin (SVIL). Genomics *52*, 342–351.

Porter, M. E., Scholey, J. M., Stemple, D. L., Vigers, G. P., Vale, R. D., Sheetz, M. P., and McIntosh, J. R. (1987). Characterization of the microtubule movement produced by sea urchin egg kinesin. J. Biol. Chem. *262*, 2794–2802.

Rieder, G., Tessier, A. J., Qiao, X. T., Madison, B., Gumucio, D. L., and Merchant, J. L. (2005). *Helicobacter*-induced intestinal metaplasia in the stomach correlates with Elk-1 and serum response factor induction of villin. J. Biol. Chem. *280*, 4906–4912.

Romer, L. H., Birukov, K. G., and Garcia, J. G. (2006). Focal adhesions: paradigm for a signaling nexus. Circ. Res. *98*, 606–616.

Sandilands, E., and Frame, M. C. (2008). Endosomal trafficking of Src tyrosine kinase. Trends Cell Biol. *18*, 322–329.

Seals, D. F., Azucena, E. F., Jr., Pass, I., Tesfay, L., Gordon, R., Woodrow, M., Resau, J. H., and Courtneidge, S. A. (2005). The adaptor protein Tks5/Fish is required for podosome formation and function, and for the protease-driven invasion of cancer cells. Cancer Cell *7*, 155–165.

Shinjo, K., Koland, J. G., Hart, M. J., Narasimhan, V., Johnson, D. I., Evans, T., and Cerione, R. A. (1990). Molecular cloning of the gene for the human placental GTP-binding protein Gp (G25K): identification of this GTP-binding protein as the human homolog of the yeast cell-division-cycle protein CDC42. Proc. Natl. Acad. Sci. USA. *87*, 9853–9857.

Silacci, P., Mazzolai, L., Gauci, C., Stergiopulos, N., Yin, H. L., and Hayoz, D. (2004). Gelsolin superfamily proteins: key regulators of cellular functions. Cell Mol. Life Sci. *61*, 2614–2623.

Sohail, A., Sun, Q., Zhao, H., Bernardo, M. M., Cho, J. A., and Fridman, R. (2008). MT4-(MMP17) and MT6-MMP (MMP25), A unique set of membrane-anchored matrix metalloproteinases: properties and expression in cancer. Cancer Metastasis Rev. *27*, 289–302.

Spinardi, L., and Marchisio, P. C. (2006). Podosomes as smart regulators of cellular adhesion. Eur. J. Cell Biol. *85*, 191–194.

Stendahl, O. I., Hartwig, J. H., Brotschi, E. A., and Stossel, T. P. (1980). Distribution of actin-binding protein and myosin in macrophages during spreading and phagocytosis. J. Cell Biol. *84*, 215–224.

Stone, K. R., Mickey, D. D., Wunderli, H., Mickey, G. H., and Paulson, D. F. (1978). Isolation of a human prostate carcinoma cell line (DU 145). Int. J Cancer *21*, 274–281.

Stylli, S. S., Kaye, A. H., and Lock, P. (2008). Invadopodia: At the cutting edge of tumour invasion. J. Clin. Neurosci. *15*, 725–737.

Takizawa, N., Ikebe, R., Ikebe, M., and Luna, E. J. (2007). Supervillin slows cell spreading by facilitating myosin II activation at the cell periphery. J. Cell Sci. *120*, 3792–3803.

Takizawa, N., Smith, T. C., Nebl, T., Crowley, J. L., Palmieri, S. J., Lifshitz, L. M., Ehrhardt, A. G., Hoffman, L. M., Beckerle, M. C., and Luna, E. J. (2006). Supervillin modulation of focal adhesions involving TRIP6/ZRP-1. J. Cell Biol. *174*, 447–458.

Tang, B., Vu, M., Booker, T., Santner, S. J., Miller, F. R., Anver, M. R., and Wakefield, L. M. (2003). TGF-beta switches from tumor suppressor to pro-metastatic factor in a model of breast cancer progression. J. Clin. Invest. *112*, 1116–1124.

Tehrani, S., Tomasevic, N., Weed, S., Sakowicz, R., and Cooper, J. A. (2007). Src phosphorylation of cortactin enhances actin assembly. Proc. Natl. Acad. Sci. USA *104*, 11933–11938.

Thalmann, G. N., Anezinis, P. E., Chang, S. M., Zhau, H. E., Kim, E. E., Hopwood, V. L., Pathak, S., von Eschenbach, A. C., and Chung, L. W. (1994). Androgen-independent cancer progression and bone metastasis in the LNCaP model of human prostate cancer. Cancer Res. *54*, 2577–2581.

Toba, S., and Toyoshima, Y. Y. (2004). Dissociation of double-headed cytoplasmic dynein into single-headed species and its motile properties. Cell Motil. Cytoskeleton *58*, 281–289.

Togo, T., and Steinhardt, R. A. (2004). Nonmuscle myosin IIA and IIB have distinct functions in the exocytosis-dependent process of cell membrane repair. Mol. Biol. Cell *15*, 688–695.

Towbin, H., Stahelin, T., and Gordon, J. (1979). Electrophoretic transfer of proteins from polyacrylamide gels to nitrocellulose sheets: procedure and some applications. Proc. Natl. Acad. Sci. USA *76*, 4350–4354.

Van den Abbeele, A., De Corte, V., Van Impe, K., Bruyneel, E., Boucherie, C., Bracke, M., Vandekerckhove, J., and Gettemans, J. (2007). Downregulation of gelsolin family proteins counteracts cancer cell invasion in vitro. Cancer Lett. *255*, 57–70.

Watanabe, S., Mabuchi, K., Ikebe, R., and Ikebe, M. (2006). Mechanoenzymatic characterization of human myosin Vb. Biochemistry *45*, 2729–2738.

Watari, A., *et al*. (2006). Suppression of tumorigenicity, but not anchorage independence, of human cancer cells by new candidate tumor suppressor gene CapG. Oncogene *25*, 7373–7380.

Weaver, A. M. (2006). Invadopodia: specialized cell structures for cancer invasion. Clin. Exp. Metastasis *23*, 97–105.

Weaver, A. M. (2008). Cortactin in tumor invasiveness. Cancer Lett. *265*, 157–166.

Webb, B. A., Eves, R., and Mak, A. S. (2006a). Cortactin regulates podosome formation: roles of the protein interaction domains. Exp. Cell Res. *312*, 760–769.

Webb, B. A., Jia, L., Eves, R., and Mak, A. S. (2007). Dissecting the functional domain requirements of cortactin in invadopodia formation. Eur. J. Cell Biol. *86*, 189–206.

Webb, B. A., Zhou, S., Eves, R., Shen, L., Jia, L., and Mak, A. S. (2006b). Phosphorylation of cortactin by p21-activated kinase. Arch. Biochem. Biophys. *456*, 183–193.

Woehlke, G., Ruby, A. K., Hart, C. L., Ly, B., Hom-Booher, N., and Vale, R. D. (1997). Microtubule interaction site of the kinesin motor. Cell *90*, 207–216.

Wu, H., and Parsons, J. T. (1993). Cortactin, an 80/85-kilodalton pp60src substrate, is a filamentous actin-binding protein enriched in the cell cortex. J. Cell Biol. *120*, 1417–1426.

Wulfkuhle, J. D., Donina, I. E., Stark, N. H., Pope, R. K., Pestonjamasp, K. N., Niswonger, M. L., and Luna, E. J. (1999). Domain analysis of supervillin, an F-actin bundling plasma membrane protein with functional nuclear localization signals. J. Cell Sci. *112*, 2125–2136.

Yamaguchi, H., and Condeelis, J. (2007). Regulation of the actin cytoskeleton in cancer cell migration and invasion. Biochim. Biophys. Acta *1773*, 642–652.

Yamaguchi, H., *et al*. (2005). Molecular mechanisms of invadopodium formation: the role of the N-WASP-Arp2/3 complex pathway and cofilin. J. Cell Biol. *168*, 441–452.

Yi, J., Kloeker, S., Jensen, C. C., Bockholt, S., Honda, H., Hirai, H., and Beckerle, M. C. (2002). Members of the Zyxin family of LIM proteins interact with members of the p130Cas family of signal transducers. J. Biol. Chem. *277*, 9580–9589.

Zaidel-Bar, R., Cohen, M., Addadi, L., and Geiger, B. (2004). Hierarchical assembly of cell-matrix adhesion complexes. Biochem. Soc. Trans. *32*, 416–420.

Zamir, E., Katz, B. Z., Aota, S., Yamada, K. M., Geiger, B., and Kam, Z. (1999). Molecular diversity of cell-matrix adhesions. J. Cell Sci. *112*, 1655–1669.